AD-A195 104 DIELECTRIC MILLIMETER WAVEGUIDES; A FEASIBILITY STUDY FOR A NOVEL DIELECT..(U) DAYTON UNIV OH C V SMITH ET AL. MAR 88 RADC-TR-88-32-VOL-2 1/1

UNCLASSIFIED F30602-81-C-0206 F/G 9/1 NL

END
DATE FILMED
9 88

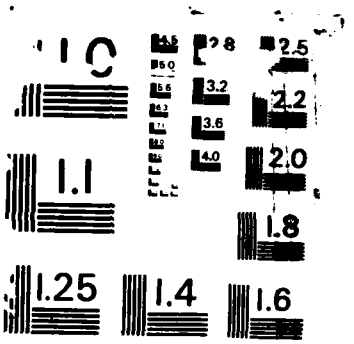

COPY RESOLUTION TEST CHART
NATIONAL BUREAU OF STANDARDS-1963-A

RADC-TR-88-32, Vol II (of two)
Final Technical Report
March 1988

DIELECTRIC MILLIMETER WAVEGUIDES
A Feasibility Study for a Novel Dielectric Millimeter Waveguide

University of Texas at Arlington

Charles V. Smith, Jr. and Jonathan S. Bagby

APPROVED FOR PUBLIC RELEASE; DISTRIBUTION UNLIMITED.

This effort was funded totally by the Laboratory Director's fund.

ROME AIR DEVELOPMENT CENTER
Air Force Systems Command
Griffiss Air Force Base, NY 13441-5700

This report has been reviewed by the RADC Public Affairs Office (PA) and is releasable to the National Technical Information Service (NTIS). At NTIS it will be releasable to the general public, including foreign nations.

RADC-TR-32, Vol II (of two) has been reviewed and is approved for publication.

APPROVED:

James C Sethares

JAMES C. SETHARES
Project Engineer

APPROVED:

John K. Schindler

JOHN K. SCHINDLER
Acting Director of Electromagnetics

FOR THE COMMANDER:

John A. Ritz

JOHN A. RITZ
Directorate of Plans and Programs

If your address has changed or if you wish to be removed from the RADC mailing list, or if the addressee is no longer employed by your organization, please notify RADC (EEAC) Hanscom AFB MA 01731-5000. This will assist us in maintaining a current mailing list.

Do not return copies of this report unless contractual obligations or notices on a specific document requires that it be returned.

UNCLASSIFIED
SECURITY CLASSIFICATION OF THIS PAGE

AD-A195 104

REPORT DOCUMENTATION PAGE

Form Approved OMB No. 0704-0188

1a. REPORT SECURITY CLASSIFICATION UNCLASSIFIED	1b. RESTRICTIVE MARKINGS N/A
2a. SECURITY CLASSIFICATION AUTHORITY N/A	3. DISTRIBUTION / AVAILABILITY OF REPORT Approved for public release; distribution unlimited.
2b. DECLASSIFICATION / DOWNGRADING SCHEDULE N/A	
4. PERFORMING ORGANIZATION REPORT NUMBER(S) N/A	5. MONITORING ORGANIZATION REPORT NUMBER(S) RADC-TR-88-32, Vol II (of two)
6a. NAME OF PERFORMING ORGANIZATION University of Texas at Arlington	6b. OFFICE SYMBOL (If applicable)
6c. ADDRESS (City, State, and ZIP Code) Dept of E.E. P.O. Box 19016 Arlington TX 76019	7a. NAME OF MONITORING ORGANIZATION Rome Air Development Center (EEAC) 7b. ADDRESS (City, State, and ZIP Code) Hanscom AFB MA 01731-5000
8a. NAME OF FUNDING / SPONSORING ORGANIZATION Rome Air Development Center	8b. OFFICE SYMBOL (If applicable) EEAC
8c. ADDRESS (City, State, and ZIP Code) Hanscom AFB MA 01731-5000	9 PROCUREMENT INSTRUMENT IDENTIFICATION NUMBER F30602-81-C-0206 10. SOURCE OF FUNDING NUMBERS

PROGRAM ELEMENT NO	PROJECT NO.	TASK NO	WORK UNIT ACCESSION NO.
61101F	LDFP	03	P6

11. TITLE (Include Security Classification)
DIELECTRIC MILLIMETER WAVEGUIDES A FEASIBILITY STUDY FOR A NOVEL DIELECTRIC MILLIMETER WAVEGUIDE

12. PERSONAL AUTHOR(S)
Charles V. Smith, Jr. and Jonathan S. Bagby

13a. TYPE OF REPORT	13b. TIME COVERED	14. DATE OF REPORT (Year, Month, Day)	15. PAGE COUNT
Final	FROM Mar 86 TO Feb 87	March 1988	62

16. SUPPLEMENTARY NOTATION
Proj I.D.: Dielectric Mill Waveguide - I, UCLA; Dielectric Mill Waveguide - II, Univ of Texas
This effort was funded totally by the Laboratory Director's funds.

17. COSATI CODES			18. SUBJECT TERMS (Continue on reverse if necessary and identify by block number)
FIELD	GROUP	SUB-GROUP	
17			Dielectric Waveguides Millimeter Waves

19. ABSTRACT (Continue on reverse if necessary and identify by block number)

This is a final report of an initial research to theoretically access engineering feasibility of manufacturing low cost, low loss millimeter (10mm-1mm) waveguide systems using methods from fiber optics research developed for production of glass fiber lightguides. The research completed as of this reporting indicates the following:

1. There exist low loss, approximately 10% of center frequency bandwidth TE propagation modes for the guides as proposed.
2. The structures tend to be excessively large in transverse dimensions at the longer wavelengths; however, as expected, the structures appear to be of a very desirable size at the short wavelengths.
3. The materials data is difficult to obtain and substantiate because of the proprietary nature associated with material development and the technical difficulty in making suitable measurements at the proposed frequencies.

20. DISTRIBUTION / AVAILABILITY OF ABSTRACT	21. ABSTRACT SECURITY CLASSIFICATION
☒ UNCLASSIFIED/UNLIMITED ☐ SAME AS RPT ☐ DTIC USERS	UNCLASSIFIED
22a. NAME OF RESPONSIBLE INDIVIDUAL JAMES C. SETHARES	22b. TELEPHONE (Include Area Code) (617) 377-4663
	22c. OFFICE SYMBOL RADC/EEAC

DD Form 1473, JUN 86 — Previous editions are obsolete. SECURITY CLASSIFICATION OF THIS PAGE

UNCLASSIFIED

CONTENTS

I. IDENTIFICATION AND SIGNIFICANCE OF RESEARCH OBJECTIVE

The research objective is to theoretically assess engineering feasibility of manufacturing low cost, low loss millimeter waveguide systems (10 mm - 1 mm) using methods from fiber optics research developed for production of glass fiber lightguides. To more completely utilize such optical fiber construction concepts, the initial research effort was a theoretical study of graded index of refraction Solid Guides of circular cross section and O-type Guides [1,2] of circular cross section with a graded index of refraction wall. More complex wave guiding structures such as non-circular cross sections (e.g., elliptical), could be manufactured using these techniques.

A number of significant technologies can be implemented upon the successful development of low cost, low loss millimeter waveguide systems. These technologies include wide bandwidth communications links which can be EMP hardened; small,lightweight radars for autonomously guided weapons and area surveillance using imaging-mode operation; sensors for robotics application; and free space, line of sight communications systems (e.g., man to man, aircraft to aircraft, ship to ship, etc.) offering security and antijam capability. A further significant advantage

for such low cost, low loss millimeter waveguide systems is the possibility of developing analog signal processing devices of reasonable size, including periodic structure [3] and transversal filters [4]. In fact, the original realization of the transversal filter was implemented with coaxial cable. The implication is that systems operating at these wavelengths with low loss waveguides can achieve signal processing without conversion to an intermediate frequency.

II. TECHNICAL SUMMARY

For millimeter wavelength systems (10 mm - 1.0 mm), guides are presently fabricated to high mechanical precision, usually out of costly materials such as coin silver. Costs for such guides is in the order $500 per meter of transmission link run if the number of connections is small; and, the advantage afforded by operation at these smaller wavelengths is lost by the large, poor form factor assemblies presently used. What was proposed is to adapt the construction techniques developed by workers in fiber optics [5,6] to manufacture low loss graded index of refraction Solid Guides and O-type Guides with a graded index of refraction wall suitable for use at millimeter wavelengths. In this process a preform of the desired cross section parameter variation is manufactured using chemical vapor deposition and is drawn to the desired diameter; for optical fiber waveguides, dimensions are held to within one percent for fibers five thousandths of an inch in diameter. Such mechanical precision should also be obtained in the manufacture of millimeter waveguides by a similar process. The techniques of drawing the waveguides as is done for optical fibers should lead to significant reduction in production cost while maintaining the

mechanical precision required. Further, initial considerations indicate the possibility of a significant reduction in the propagation attenuation. Available rectangular metal pipe waveguides such as WR5 (RG135/U) have attenuations of the order 25 dB per meter; in contrast, results from this study show that a few tenths of a dB per meter attenuation are readily attainable for millimeter wavelength operation in guides constructed of low loss dielectric materials such as water-free fused silica (Thermal American Fused Quartz "spectrasil") and that lower values may be achieved. It is noteworthy that 1 dB per meter at one millimeter wavelength corresponds to a figure of merit of 1000 wavelengths per dB of attenuation, a figure of merit indicating the suitability of the transmission medium for utilization in realization of transversal filters; corresponding values for other transversal filter realizations media are 1000-5000 for SAW, 500 for MSW and 500 for copper guide at microwave frequencies. Since attenuations of much less than 1dB per meter can be attained in the proposed guides, this propagation medium approaches and exceeds the figure of merit of SAW for transversal filters.

III. DESIGN GUIDELINES

In this section we develop the basic design criteria used in our design for the O-type millimeter waveguide. The basic structure under consideration is shown in Figure 1. We begin by developing a simple transmission line analogy, and then move on to the design strategy for the millimeter waveguide.

A. Transmission Line Analogy

Here we develop criteria for maximization of voltage reflection from a simple alternating, multi-section transmission line circuit. The results are useful in formulating analogous criteria for maximization of electromagnetic wave reflection from alternating multi-layered dielectric structures.

Consider the alternating multi-section transmission line circuit shown in Figure 2a. It consists of a source with internal impedance Z_s connected to a load of impedance Z_ℓ via N transmission line segments. The transmission line segments have alternating characteristic impedances Z_{01} and Z_{02}, and are of alternating lengths $\lambda_1/4$ and $\lambda_2/4$, where λ_1 and λ_2 are the wavelengths in the alternating sections.

Using elementary transmission line analysis it can be shown that the input impedance seen by the source is given by

$$Z_i = Z_\ell \left(\frac{Z_{01}}{Z_{02}}\right)^N$$

so that if $Z_{01} \neq Z_{02}$ and N is large we have either an extremely large or extremely small input impedance. Now the voltage reflection coefficient at the source is given by

$$\Gamma_i = \frac{Z_i - Z_s}{Z_i + Z_s}$$

which has a magnitude very close to one if N is large.

By this analysis we see that the voltage reflection coefficient can be maximized by: 1) increasing the <u>contrast</u> between the characteristic impedances Z_{01} and Z_{02}, and 2) increasing the <u>number</u> <u>N</u> of transmission line sections.

B. <u>Design Parameters</u>

In designing our millimeter waveguide we will adapt these rules for maximizing the reflection of electromagnetic waves inside of the guide.

We will concentrate on structures with alternating wall composition and thickness. The wall thicknesses will be chosen to be a quarter wavelength in thickness for waves of frequency f_0 incident on the wall at angle of incidence θ_0. Referring to Figure 2b, this means that

$$t_i = \frac{\lambda_0}{4\,\varepsilon_{ri}\cos\theta_i}$$

where $\lambda_0 = c/f$, $\varepsilon_i = \varepsilon_{ri}\varepsilon_0$, and by Snell's law

$$\theta_i = \sin^{-1}(\sin\theta_0/\,\varepsilon_{ri})$$

We will use as our standard test case in the rest of this document the following parameters:

f_0 = 100 GHz, θ_0 = 80 degrees

ε_{r1} = 3.285, $\varepsilon_{r2} = 1.2\varepsilon_{r1}$ = 3.942

N = 16, 32, 64 layers

IV. REFLECTION FROM LAYERED STRUCTURES

In this section we develop two methods of finding the reflection coefficient of plane electromagnetic waves of arbitrary frequency and polarization incident at any angle on a infinite planar layered dielectric structure. We first restrict our analysis to lossless dielectrics here; later the results will be generalized to lossy dielectrics. These results will be used later in our analysis of wave guidance by a multi-layered dielectric planar waveguide. As we will show later, this behavior of this waveguide closely approximates the behavior of the multi-layered dielectric O-type waveguide.

A. Reflection from Lossless Planar Layers

Consider the situation depicted in Figure 3. An arbitrarily polarized plane wave of magnitude A in free-space is incident on an infinite planar multi-layered dielectric structure. The structure consists of N homogeneous lossless dielectric slabs of permittivity ε_i and thickness t_i, for $i=1,\ldots,N$. We seek the magnitude of the resultant reflected wave in free-space, denoted B in Figure 3.

Following Wait [7] we can define wave impedances in each region as the ratio of the tangential electric field to the tangential magnetic field. Electromagnetic boundary conditions are then enforced by equating wave impedances on each side of each dielectric boundary. Beginning this process at the boundary at y=0 and continuing to the boundary at $y=t_N$ yields the following iterative formula for the overall reflection coefficient, defined as the ratio of B to A:

$$\Gamma = \frac{Z_{yN} - Z_0}{Z_{yN} + Z_0}$$

$$Z_{yN} = Z_N \frac{Z_{yN-1}\cos(k_{yN}t_N) + jZ_N\sin(k_{yN}t_N)}{Z_N\cos(k_{yN}t_N) + jZ_{yN-1}\sin(k_{yN}t_N)}$$

$$\vdots$$

$$Z_{yi} = Z_i \frac{Z_{yi-1}\cos(k_{yi}t_i) + jZ_i\sin(k_{yi}t_i)}{Z_i\cos(k_{yi}t_i) + jZ_{yi-1}\sin(k_{yi}t_i)}$$

$$\vdots$$

$$Z_{y1} = Z_1 \frac{Z_0\cos(k_{y1}t_1) + jZ_1\sin(k_{y1}t_1)}{Z_1\cos(k_{y1}t_1) + jZ_0\sin(k_{y1}t_1)}$$

where

$$Z_i = \begin{cases} \dfrac{\omega\mu_0}{k_{yi}} & \text{... for TE (perpendicular) polarization} \\ \dfrac{k_{yi}}{\omega\varepsilon_i} & \text{... for TM (parallel) polarization} \end{cases}$$

$$k_{yi} = k_0 \sqrt{\varepsilon_{ri} - \sin^2\theta}$$

with $\varepsilon_i = \varepsilon_{ri}\varepsilon_0$ and $k_0 = \omega/c$.

This formulation was used in the computer program REFL. This program evaluates the reflection coefficient versus angle of incidence and frequency for both polarization states. Figures 4 through 7 are graphs of sample output for the program for our standard test cases.

It is also possible to solve for the overall reflection coefficient by use of wave matrix formalism, as found in Collins [8]. If C denotes the amplitude of the wave transmitted through the multi-layered structure into free-space on the far side, it can be shown that the following matrix relation holds between A, B, and C:

$$\begin{bmatrix} A \\ B \end{bmatrix} = \frac{1}{T_0} \begin{bmatrix} 1 & R_0 \\ R_0 & 1 \end{bmatrix} \begin{bmatrix} T \end{bmatrix}_N \frac{1}{T_N} \begin{bmatrix} 1 & R_N \\ R_N & 1 \end{bmatrix} \begin{bmatrix} C \\ 0 \end{bmatrix}$$

where [T] denotes the matrix

$$T = \frac{1}{1 - R_1^2} \begin{bmatrix} e^{j(\delta_1+\delta_2)} - R_1^2 e^{j(\delta_1-\delta_2)} & 2jR_1 e^{j\delta_1} \sin \delta_2 \\ -2jR_1 e^{-j\delta_1} \sin \delta_2 & e^{-j(\delta_1+\delta_2)} - R_1^2 e^{-j(\delta_1-\delta_2)} \end{bmatrix}$$

Here

$$R_0 = \frac{Z_1 - Z_0}{Z_1 + Z_0} \qquad R_1 = \frac{Z_1 - Z_2}{Z_1 + Z_2} \qquad R_N = \frac{Z_0 - Z_2}{Z_0 + Z_2}$$

with Z_i defined as above, and $\delta_i = k_{yi} t_i$.

In order to use this formulation to find the overall reflection coefficient we must have an efficient way to raise the matrix [T] to large powers.

Sylvester's theorem as outlined in Collins [8] allows us to express [T] raised to the N power in terms of the sum of two matrices multiplied by powers of eigenvalues of the original matrix. This means that calculation of [T] to arbitrarily high powers can be accomplished by addition of two matrices, resulting in a vast savings of time when N is large.

This technique of computing the reflection coefficient versus angle of incidence and frequency was implemented in the computer program WMAT. Output of the program is indistinguishable from that provided in Figures 4 through 7.

B. Reflection from Lossless Cylindrical Layers

In this section we use the wave impedance technique introduced in the previous section to solve for the reflection coefficient for cylindrical waves of arbitrary frequency and polarization incident at any angle on a multi-layered cylindrical structure. Once again we derive results for the lossless case, which will be generalized to the lossy case later on.

Consider the situation depicted in Figure 8. An arbitrarily polarized cylindrical wave of amplitude A is incident at angle θ on an infinitely-long cylindrical structure. The structure is composed of N concentric homogeneous dielectric layers of permittivity ε_i and inner radius ρ_i, where i=1,...,N. We seek the magnitude B of the resultant reflected cylindrical wave.

Once again we define the wave impedances in each layer as the ratio of total tangential electric field to total tangential magnetic field, and enforce boundary conditions by equating wave impedances on both sides of each boundary. This process yields an interative formula for the overall reflection coefficient. In the case of TM polarization of the incident wave, we obtain

$$\Gamma = \frac{Z_0 H_n^{(2)}(k_{\rho 0}\rho_N) - Z_{\rho N} H_n^{(2)\prime}(k_{\rho 0}\rho_N)}{Z_{\rho N} H_n^{(1)\prime}(k_{\rho 0}\rho_N) - Z_0 H_n^{(1)}(k_{\rho 0}\rho_N)}$$

$$Z_{\rho N} = Z_N \frac{H_n^{(2)}(k_{\rho N}\rho_N) + K_{N-1}H_n^{(1)}(k_{\rho N}\rho_N)}{H_n^{(2)\prime}(k_{\rho N}\rho_N) + K_{N-1}H_n^{(1)\prime}(k_{\rho N}\rho_N)}$$

$$\vdots$$

$$K_i = \frac{Z_{i+1}H_n^{(2)}(k_{\rho i+1}\rho_i) - Z_{\rho i}H_n^{(2)\prime}(k_{\rho i}\rho_i)}{Z_{\rho i}H_n^{(1)\prime}(k_{\rho i+1}\rho_i) - Z_{i+1}H_n^{(1)}(k_{\rho i+1}\rho_i)}$$

$$Z_{\rho i} = Z_i \frac{H_n^{(2)}(k_{\rho i}\rho_i) + K_{i-1}H_n^{(1)}(k_{\rho i}\rho_i)}{H_n^{(2)\prime}(k_{\rho i}\rho_i) + K_{i-1}H_n^{(1)\prime}(k_{\rho i}\rho_i)}$$

$$\vdots$$

$$K_0 = \frac{Z_1H_n^{(2)}(k_{\rho 1}\rho_0) - Z_{\rho 0}H_n^{(2)\prime}(k_{\rho 1}\rho_0)}{Z_{\rho 0}H_n^{(1)\prime}(k_{\rho 1}\rho_0) - Z_1H_n^{(1)}(k_{\rho 1}\rho_0)}$$

$$Z_{\rho 0} = Z_0 \frac{H_n^{(2)}(k_{\rho 0}\rho_0)}{H_n^{(2)\prime}(k_{\rho 0}\rho_0)}$$

where $H_n^{(1)}$ and $H_n^{(2)}$ are Hankel functions of the first and second kind of order n, and primes denote derivatives with respect to argument. The TM wave impedances are defined by

$$Z_i = \frac{k_{\rho i}}{\omega\varepsilon_i} \qquad k_{\rho i} = k_0\sqrt{\varepsilon_{ri} - \sin^2\theta_0}$$

and the order n denotes the angular variation $e^{jn\phi}$ of the incident and reflected fields (usually taken as zero).

In the case of a TE polarized incident field, a similar derivation yields

$$\Gamma = \frac{Z_0 H_n^{(2)'}(k_{\rho 0}\rho_N) - Z_{\rho N} H_n^{(2)}(k_{\rho 0}\rho_N)}{Z_{\rho N} H_n^{(1)}(k_{\rho 0}\rho_N) - Z_0 H_n^{(1)'}(k_{\rho 0}\rho_N)}$$

$$Z_{\rho N} = Z_N \frac{H_n^{(2)'}(k_{\rho N}\rho_N) + K_{N-1} H_n^{(1)'}(k_{\rho N}\rho_N)}{H_n^{(2)}(k_{\rho N}\rho_N) + K_{N-1} H_n^{(1)}(k_{\rho N}\rho_N)}$$

$$\vdots$$

$$K_i = \frac{Z_{i+1} H_n^{(2)'}(k_{\rho i+1}\rho_i) - Z_{\rho i} H_n^{(2)}(k_{\rho i 1}\rho_i)}{Z_{\rho i} H_n^{(1)}(k_{\rho i+1}\rho_i) - Z_{i+1} H_n^{(1)'}(k_{\rho i+1}\rho_i)}$$

$$Z_{\rho i} = Z_i \frac{H_n^{(2)'}(k_{\rho i}\rho_i) + K_{i-1} H_n^{(1)'}(k_{\rho i}\rho_i)}{H_n^{(2)}(k_{\rho i}\rho_i) + K_{i-1} H_n^{(1)}(k_{\rho i}\rho_i)}$$

$$\vdots$$

$$K_0 = \frac{Z_1 H_n^{(2)'}(k_{\rho 1}\rho_0) - Z_{\rho 0} H_n^{(2)}(k_{\rho 1}\rho_0)}{Z_{\rho 0} H_n^{(1)}(k_{\rho 1}\rho_0) - Z_1 H_n^{(1)'}(k_{\rho 1}\rho_0)}$$

$$Z_{\rho 0} = Z_0 \frac{H_n^{(2)'}(k_{\rho 0}\rho_0)}{H_n^{(2)}(k_{\rho 0}\rho_0)}$$

with the TE wave impedance defined by

$$Z_i = \frac{\omega \mu_0}{k_{\rho i}}$$

where $k_{\rho i}$ is given as above.

This technique of finding the reflection coefficient versus angle of incidence and frequency was implemented in the computer program CYL. Graphical results of this program are provided in Figures 9 and 10.

Note that the curves for this cylindrical case are very close to the curves in the planar case when the curvature of the cylinder is on the order of a wavelength or more. This result implies that we can use the simpler planar case as a close approximation to the actual cylindrical guide.

C. Reflection from Lossy Layers

In this section we generalize the formulations of the previous sections to obtain reflection coefficients for lossy dielectric layers. We first consider the planar case, and then the cylindrical case.

The generalization to lossy dielectrics in the planar case is a trivial one. All of the previous results hold in the lossy case if we replace the permittivity ε everywhere by the complex permittivity,

$$\varepsilon_c = \varepsilon' - j\varepsilon''$$

where ε' is the real permittivity and ε'' is the loss tangent of the dielectric. The loss tangent can also be written in terms of the conductivity of the dielectric as $\varepsilon'' = \sigma/\omega$.

This generalization was incorporated into the wave impedance formulation for the reflection coefficient from planar layers. The modified program LREFL computes the reflection coefficient versus angle of incidence and frequency in the lossy case. Sample output from the program is provided in Figure 11.

The generalization to lossy dielectrics in the cylindrical case is obtained in exactly the same way as above. One added complication, however, is the requirement for computation of Hankel functions of complex arguments.

The program LCYL computes the reflection coefficient versus angle of incidence and frequency in the lossy case. Sample output of the program is provided in Figure 12.

V. WAVEGUIDE ATTENUATION CALCULATION

In this section we use the results of the previous sections to calculate the attenuation of electromagnetic waves guided by layered structures. We restrict our attention to the planar case; extension to the cylindrical case is discussed in the next section.

A. Approximate Loss Calculation

An simple, approximate waveguide loss calculation can be obtained as follows.

Consider a plane wave of frequency f bouncing at an angle θ down the interior of the planar layered structure as shown in Figure 13. Successive reflections occur at a distance d apart, and at each reflection the magnitude of the wave is decreased by the multiplicative factor $|R|$, which is the magnitude of the reflection coefficient. If we assume that the wave is decreasing with distance in the form $e^{-\alpha z}$, then we can solve for α as

$$\alpha = -\ln(|R|)/d \quad \text{Np/m}$$

Using the fact that $d = t \tan\theta$ and 1 Np/m = 8.686 dB/m, we obtain

$$\alpha = -8.686 \frac{\ln(|R|)}{t \tan\theta}$$

Sample values of α for the test cases are provided in Table 1.

It should be noted carefully that this calculation is a very rough one due to numerous approximations being used. They are:

1. We have assumed that the wave being guided is a single plane wave. A better approximation is obtianed by assuming that the field in the guide is the sum of several plane waves superimposed. However, even this yields approximate results, since we have no guarantee that the waves guided by this structure are plane waves.

2. We have assumed that we know a-priori the angle and frequency of propagation in the waveguide. It is entirely possible that the dominant mode in the guide might have another frequency and might bounce down the guide at another angle.

B. Exact Dispersion Calculation

A more exact analysis of the dispersion of the planar guide is provided here. We will make use of an equivalent guide, and solve exactly for the dispersion relation of this equivalent

guide.

Given the complex reflection coefficient R for plane waves incident on a homogeneous material at the angle θ, we can compute the permittivity and conductivity of the material. A simple calculation shows

$$\varepsilon_r = \sin^2\theta + \cos^2\theta \, \mathrm{Re}\left(\frac{1 - R}{1 + R}\right)^2$$

$$\sigma = -\omega\varepsilon_0\cos^2\theta \, \mathrm{Im}\left(\frac{1 - R}{1 + R}\right)^2$$

where Re and Im denote the real and imaginary parts, respectively.

Now consider the propagation of electromagnetic waves in the situation depicted in Figure 14. It can be shown that the propagation constant for this system satisfies the following characteristic equation:

$$(k_{y0}^2 + k_y^2)\sin(k_{y0}t) = 2jk_{y0}k_y\cos(k_{y0}t)$$

where

$$k_{y0} = \sqrt{k_0^2 - \zeta^2}, \quad k_y = \sqrt{\varepsilon_c k_0^2 - \zeta^2}$$

with ζ the complex propagation constant for the waveguide.

This formulation was used to calculate ζ for the planar layered guide, and the resultant dispersion curves produced by the program DISP are given in Figures 15 and 16.

VI. REFLECTION COEFFICIENT BY RAY TRACING

A computer program based on a ray tracing - transmission line technique has been developed to calculate the reflection coefficient of a multiple layer, planar, dielectric waveguiding structure. The computer program calculates the amplitude and phase shift of the reflection coefficient at the input wall for any number of dielectric layers as a function of incident angle. The data generated by this program correlates very well with waveguide algorithms developed by other members of the study group. Inputs to the program include:

* Number of Layers
* Illuminating Wave Frequency
* Illuminating Wave Angle Incidence
* Quarter Wavelength Matching Information For Layer Thickness Calculation
  1. Matched Frequency
  2. Matched Incident Angle In The Layer
  3. Layer Dielectric Coefficient
* Propagation Mode Type
  1. Transverse Electric (TE) - Perpendicular Polarization
  2. Transverse Magnetic (TM) - Parallel Polarization
* Characteristics of the Surrounding Media

The program begins by calculating the thicknesses of the dielectric layers for quarter wavelength matching at a fixed

incident angle and fixed frequency for each layer. After this calculation is completed the thicknesses are stored for later use. Snell's law is used to calculate for each incident angle of illumination the necessary incident angles of propagation in the layers. The main computation then proceeds using standard transmission line techniques. Starting at the load (non-illuminated) side of the structure the program calculates the complex reflection coefficient of each layer interface taking into account the characteristics of surrounding media (usually air) at the first (load) interface. The formula used for calculating the complex reflection coefficient depends upon the propagation characteristics (transverse electric or transverse magnetic) of the illuminating wave.

After the reflection coefficient is calculated the input impedance at the input side of the layer is computed taking into account the correct propagation distance. This is then used to calculate the reflection coefficient at the new interface. The process is repeated until the illuminated interface is arrived at. The complex reflection coefficient as a function of incident angle is then plotted.

A parallel plate waveguide using dielectric walls can be analyzed using this method. Alpha and Beta can be calculated for high values of reflection coefficient. Plots of alpha and beta at a function of frequency can then be obtained.

A. TE and TM Modes

The propagation mode types are transverse electric (TE) and transverse magnetic (TM) depending upon whether the electric vector is perpendicular or parallel to the plane of incidence. The complex reflection coefficient for these two cases are given in Section IV A of this report.

B. Transmission Line Input Impedance

The input impedance to each layer is calculated from the following familiar relation from transmission line theory,

$$Z_{in} = \frac{1 + \Gamma \exp(-j\beta d_n)}{1 - \Gamma \exp(-j\beta d_n)}$$

where Γ is the complex reflection coefficient, β is the phase constant of the wave, and d_n is the electrical path length in the layer.

C. Snell's Law For Transmission Angles

The Snell Relation gives the transmission angle to the normal at a dielectric media boundary.

D. Quarter Wavelength Layer Matching

Quarter wave matching in each layer is provided by making the layer widths such that the wave experiences a quarter wavelength propagation path at its transmission angle in the dielectric medium. The matching geometry is shown in Figure 2b.

E. Parallel Plate Waveguide Using Layered Dielectric Walls

A parallel plate waveguide using layered dielectric walls can be analyzed using this method. Alpha and beta can be arrived at for high values of reflection coefficient by the following formulas. Note that beta is a function of geometry (wall separation) only.

$$\alpha = -8.686 \frac{\ln(|R|)}{t \tan\theta}$$

$$\beta = \sqrt{\omega^2 \mu\varepsilon - (\pi/t)^2}$$

F. FORTRAN 77 COMPUTER PROGRAM

A FORTRAN 77 program for this analysis has been written for both the U.T.A. IBM Mainframe and MS-FORTRAN for use on a PC. In both cases the complex reflection coefficient is written to a data file and then imported to lotus 123 (Ver. 2) for plotting. This is possible if the data file has a .PRN extension. In the mainframe case HAYES SMARTCOM II 1200 BAUD COMMUNICATIONS software is used to downloak the data. In the MS-FORTRAN case the program generates the data file directly.

The first point of investigation into the performance of the multi-layered dielectric waveguide ws the development of its mode characteristics. Looking at a single boundary between dielectrics, the TE mode reflection is given above, where the magnetic permeability of the material is taken at unity. In the TM mode a similar expression is presented above.

The computer analysis program developed to model the reflecting wall sequentially performed an impedance transformation from the outside or load side of the multiple layered dielectric structure to the inner boundary of the reflecting wall, and at that point determined the reflection characteristic as a function of input frequency and incident

angle.

The first data was developed from a 16 layer structure with 5 percent contrast between layers, dsigned to operate at 100 GHz with an incident angle of 80 degrees. The reflection characteristics of the TE and TM modes are shown in Figure 17, demonstrating the pre-eminence of the TE mode for low grazing angles (incident angles above 80 degrees).

From this basis, invstigation into the performance of a parallel plate waveguide fabricated with layered dielectric walls began. In the case of a parallel plate guide with an air or evacuated core, a plate seperation t, operated in mode number n, the cut-off frequency of the structure is given by nc/2t, where c is the speed of light in vacuum. In such a guide the angle of incidence of the wavefront to the surface walls is given by

$$\theta_i = \cos^{-1}(nc/2ft)$$

Using these parametric expressions to derive the incident angle for a given frequency, the performance of a waveguide structure can be analyzed for a wide spectrum of input frequencies given a defined geometry specified by the layer permittivity and contrast, number of layers, design frequency and

incident angle, and the plate seperation. There is a direct relationship between the plate seperation and the design incident angle at eh design frequency that configures the guide to a particular operating point. The results of such a wide band analysis are presented in Figure 18.

The attenuation and transmission characterisics of the structure have also been observed using the expressions derived above. For the 16 the layer case the resulting attenuation and transmission curves are shown in Figures 19a and 19b.

It may be observed that the reflection characteristics of the model clearly demonstrate a harmonic character, and the guide appears to improve in performance at harmonic frequencies. Returning to the reflecting wall analysis to check this observation it was found that at low grazing angles of 10 degrees or less the performance was not degraded between a 64 layer 100 GHz design anad a 32 layer 50 GHz design, when oerating both at 100 GHz. This development shows the promise of decreased difficulty in manufacturing and correspondingly lowered production costs. These results are shown in Figures 20 and 21.

Follow on research will further investigate the considerations of geometry, harmonic operation and materials; as

well as transition into the cylindrical and elliptical waveguide structures.

VII. SUMMARY AND CONCLUSIONS

In the research reported here the original concept of using layered dielectric walls to achieve low loss propagation media for millimeter waveguide systems has been shown to be theoretically feasible.

The research completed as of this reporting indicates the following:

1. there exist low loss, approximately 10 percent of center frequency bandwidth TE propagation modes for the guides as proposed.
2. the structures tend to be excessively large in transverse dimensions at the longer wavelengths; however, as expected, the structures appear to be of a very desirable size at the short wavelengths.
3. the materials data is difficult to obtain and substantiate because of the propritary nature associated with material development and the technical difficulty in making suitable measurements at the proposed frequencies.

It is the conclusion of the researchers that these concepts should be further examined theoretically and experimentally, but

most importantly experimentally. Further, it is the strong recommendation that further research on these waveguiding structures should be focused on the spectrum above 300 GHz. This means that these very low loss waveguide modes correspond to technically useful structures at these higher frequencies. Finally, this concept is presently, to the researchers knowledge, the only viable waveguiding structure at these frequencies.

VIII. REFERENCES

1. Shigesawa, H., and Takiyama, K., Int. Conf. Submillimeter Waves Their Appl., 3rd, Dig., Guilford, SB1-3 (1978).

2. Tsuji, M., Shigesawa, H., and Takiyama, K., "Submillimeter Guided Wave Experiments with Dielectric Waveguides," Chapter 6, Infrared and Millimeter Waves, Volume 4, ed. Button, K.J. and Wiltse, J.C., New York: Academic Press, 1981.

3. Collin, R.E., Foundations for Microwave Engineering, Chapter 8, New York: McGraw-Hill, 1966.

4. Kallman, H.E., "Transversal Filters," Proc. IRE, Vol 28, 1940, pp 302 ff.

5. Partus,F.P. and Saifi, M.A., "Lightguide Preform Manufacture," The Western Electric Engineer, Vol. XXIV, No. 1, 1980, pp 38 ff.

6. Smithgall, D.H. and Myers, D.L., "Drawing Lightguide Fiber," The Western Electric Engineer, Vol. XXIV, No. 1, 1980, pp 48 ff.

7. Wait, J. R., Electromagnetic Waves in Stratified Media. New York: MacMillan, 1962.

8. Collin, R. E., Field Theory of Guided Waves. New York: McGraw-Hill, 1960.

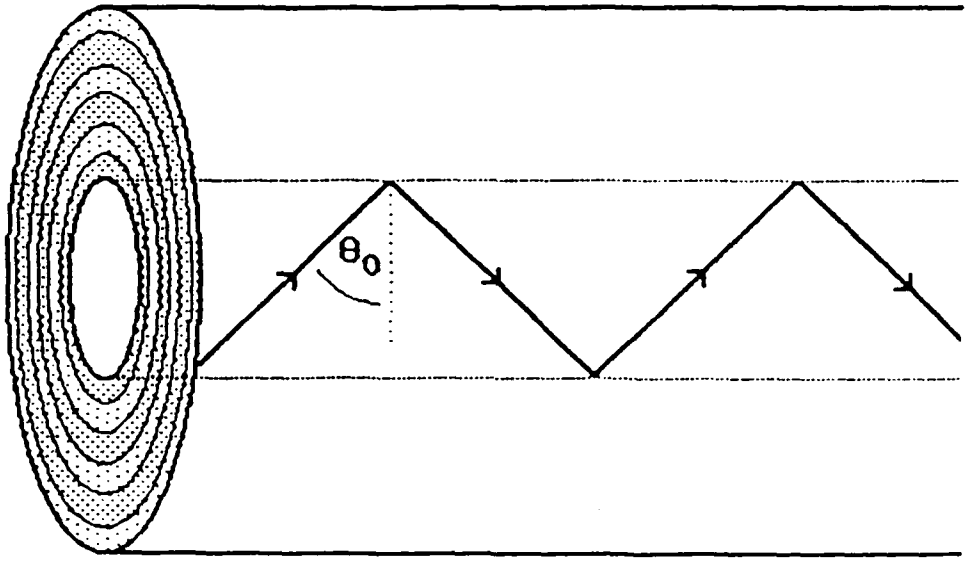

FIGURE 1.

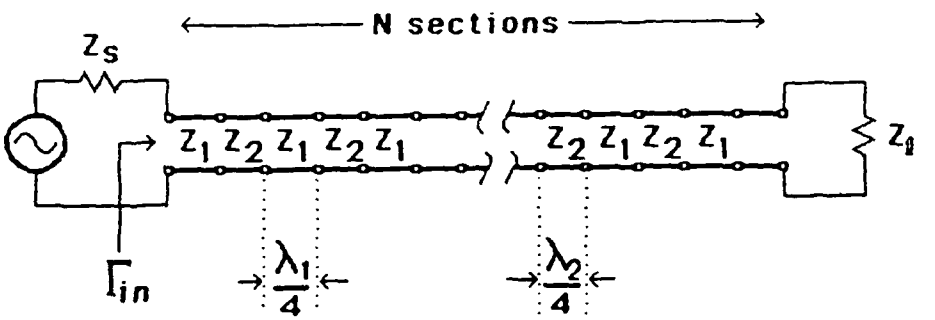

FIGURE 2a.

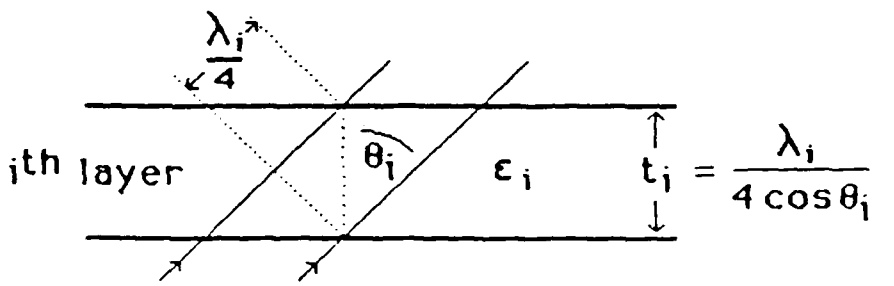

FIGURE 2b.

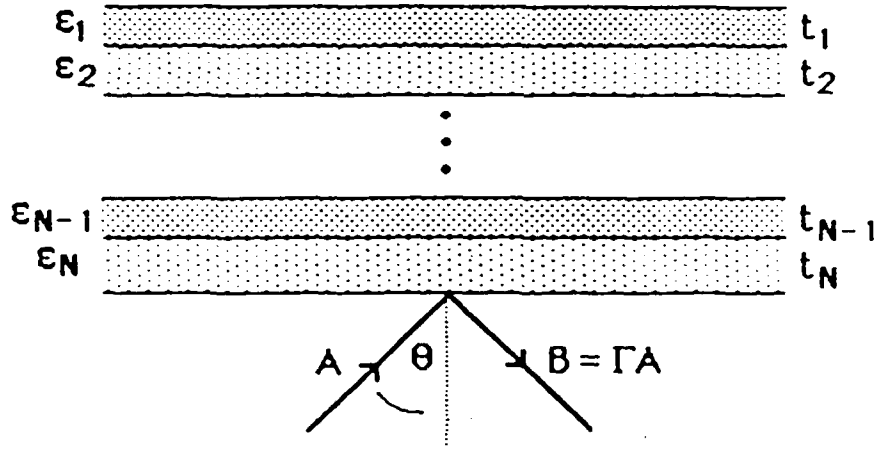
ε_1
t_1
ε_2
t_2
ε_{N-1}
t_{N-1}
ε_N
t_N
A
θ
B = ΓA

FIGURE 3.

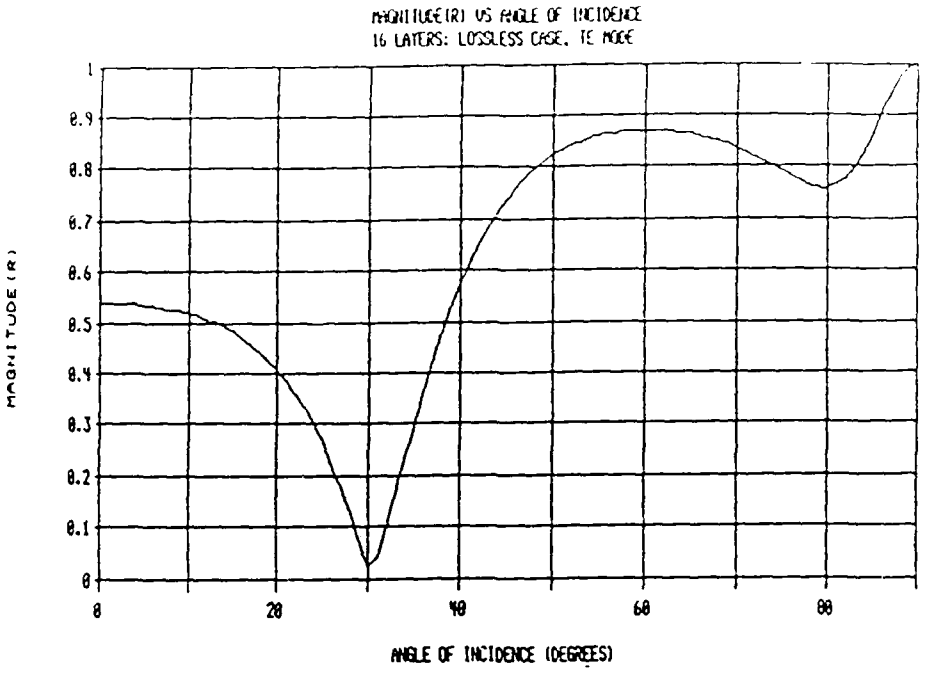
MAGNITUDE(R) VS ANGLE OF INCIDENCE
16 LAYERS: LOSSLESS CASE, TE MODE
MAGNITUDE (R)
1
0.9
0.8
0.7
0.6
0.5
0.4
0.3
0.2
0.1
0
0
20
40
60
80
ANGLE OF INCIDENCE (DEGREES)

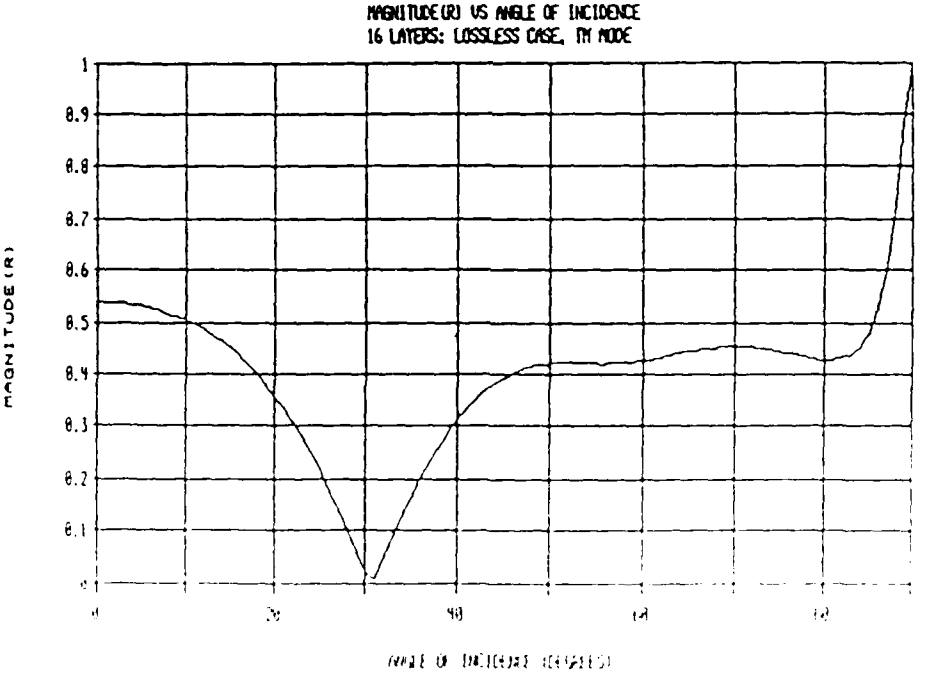
MAGNITUDE(R) VS ANGLE OF INCIDENCE
16 LAYERS: LOSSLESS CASE, TM MODE
MAGNITUDE (R)
1
0.9
0.8
0.7
0.6
0.5
0.4
0.3
0.2
0.1
0
0
20
40
60
80
ANGLE OF INCIDENCE (DEGREES)

FIGURE 4

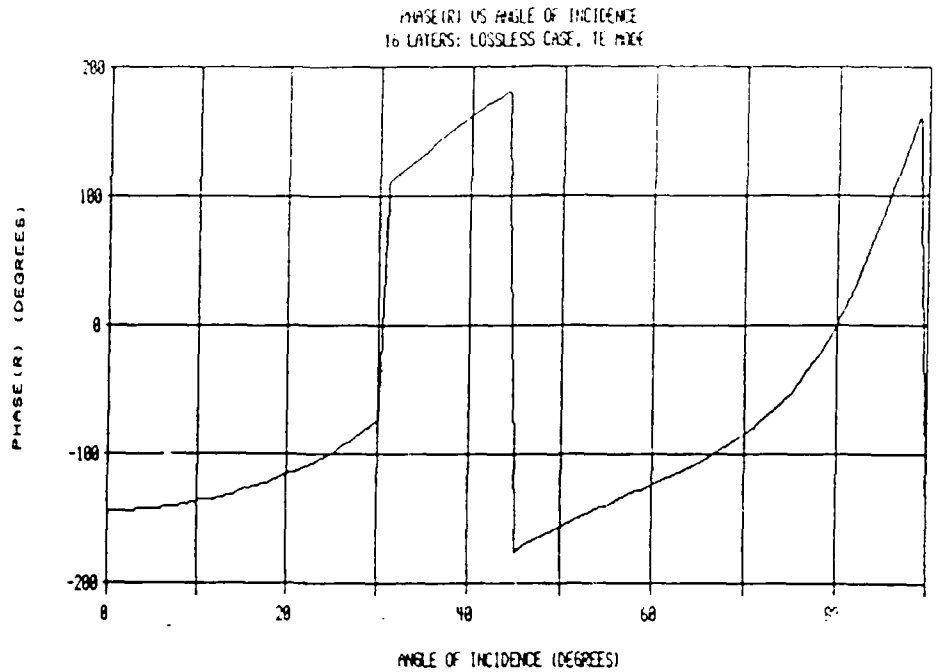
PHASE(R) VS ANGLE OF INCIDENCE
16 LAYERS: LOSSLESS CASE, TE MODE
200
100
0
-100
-200
0
20
40
60
PHASE(R) (DEGREES)
ANGLE OF INCIDENCE (DEGREES)

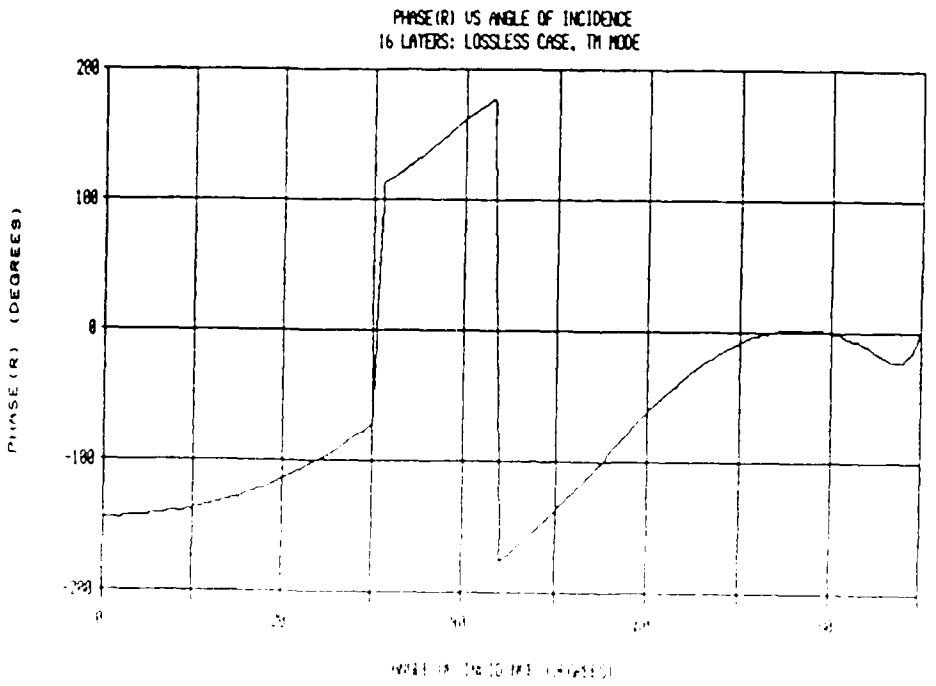
PHASE(R) VS ANGLE OF INCIDENCE
16 LAYERS: LOSSLESS CASE, TM MODE
200
100
0
-100
PHASE(R) (DEGREES)

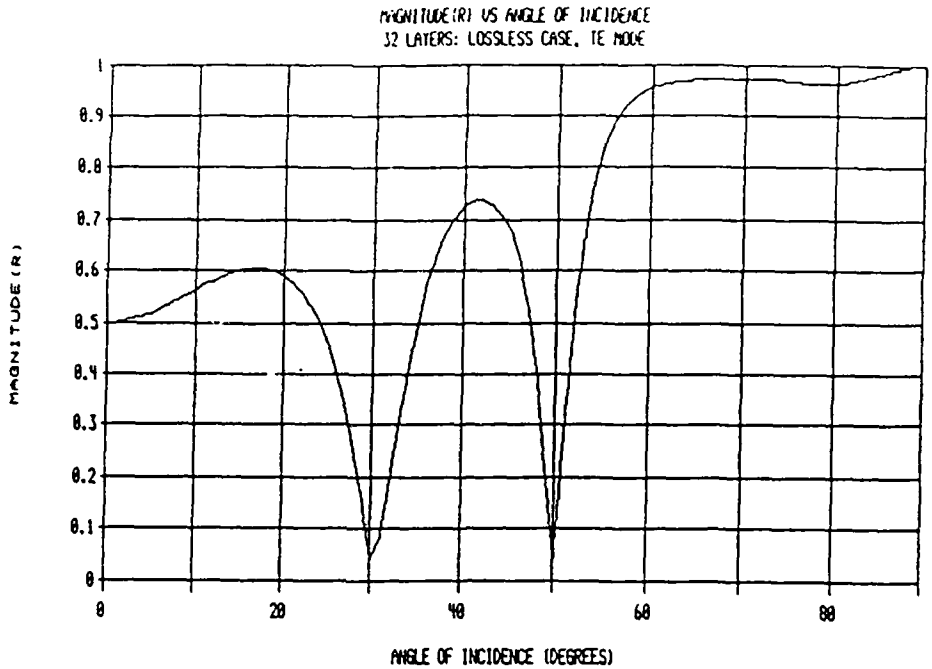
MAGNITUDE(R) VS ANGLE OF INCIDENCE
32 LAYERS: LOSSLESS CASE, TE MODE
MAGNITUDE(R)
1
0.9
0.8
0.7
0.6
0.5
0.4
0.3
0.2
0.1
0
0
20
40
60
80
ANGLE OF INCIDENCE (DEGREES)

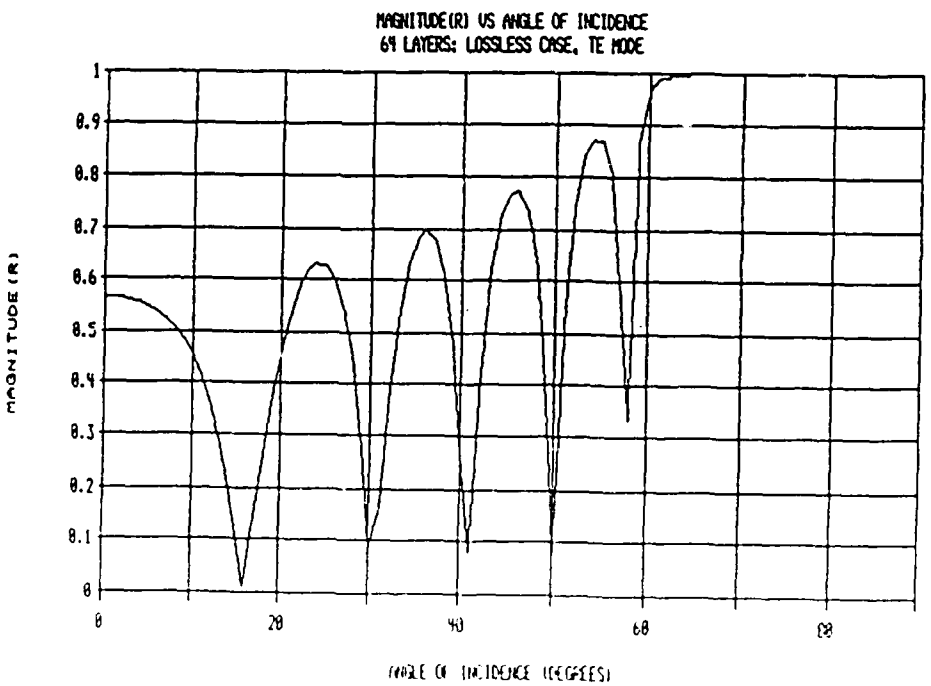
MAGNITUDE(R) VS ANGLE OF INCIDENCE
64 LAYERS: LOSSLESS CASE, TE MODE
MAGNITUDE(R)
1
0.9
0.8
0.7
0.6
0.5
0.4
0.3
0.2
0.1
0
0
20
40
60
80
ANGLE OF INCIDENCE (DEGREES)

FIGURE 6

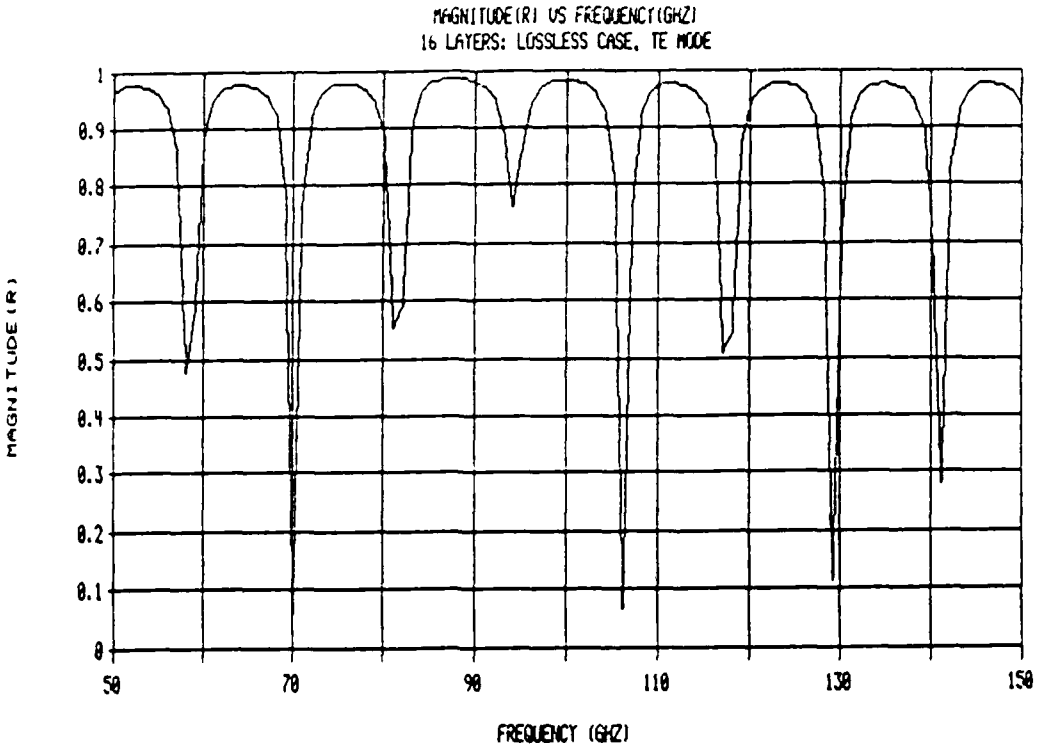
MAGNITUDE(R) VS FREQUENCY(GHZ)
16 LAYERS: LOSSLESS CASE, TE MODE
MAGNITUDE (R)
1
0.9
0.8
0.7
0.6
0.5
0.4
0.3
0.2
0.1
0
50
70
90
110
130
150
FREQUENCY (GHZ)

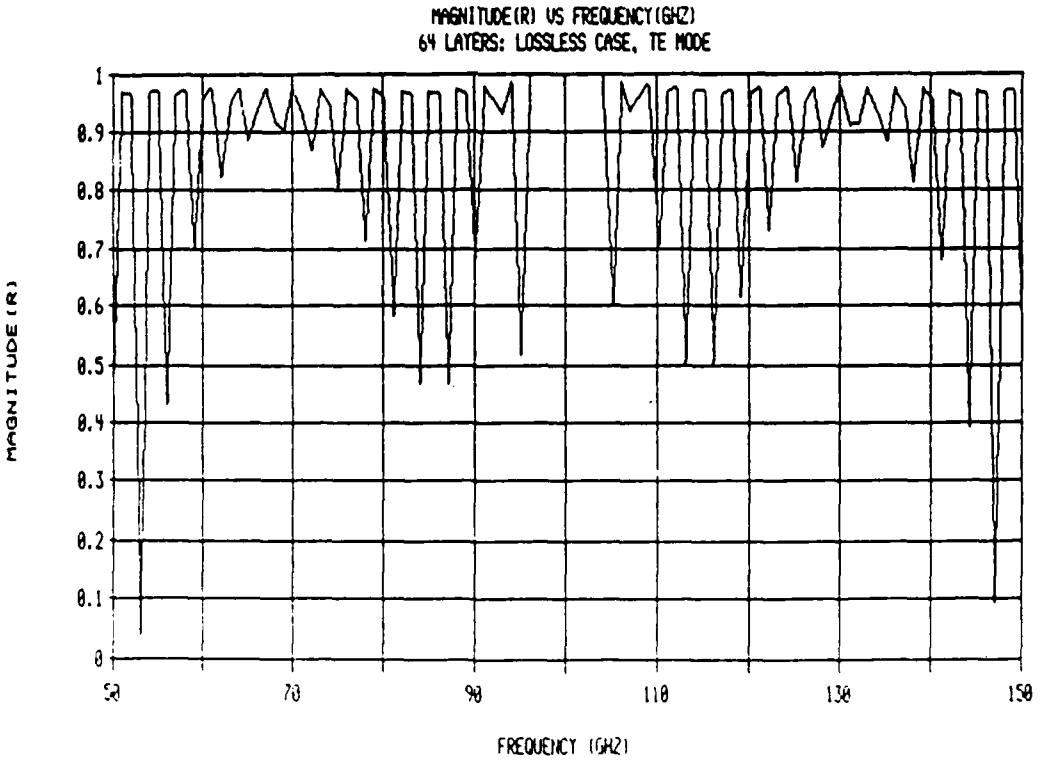
MAGNITUDE(R) VS FREQUENCY(GHZ)
64 LAYERS: LOSSLESS CASE, TE MODE
MAGNITUDE (R)
1
0.9
0.8
0.7
0.6
0.5
0.4
0.3
0.2
0.1
0
50
70
90
110
130
150
FREQUENCY (GHZ)

FIGURE 7

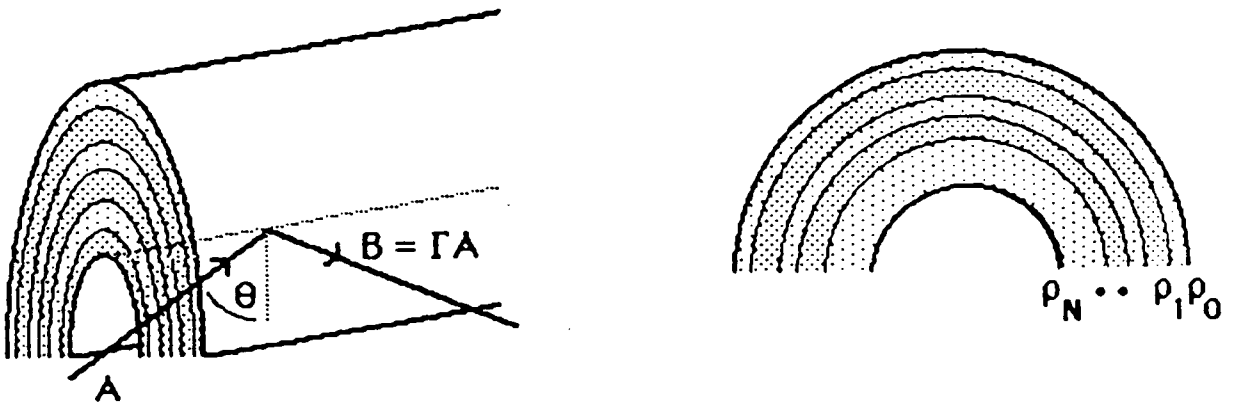

FIGURE 8

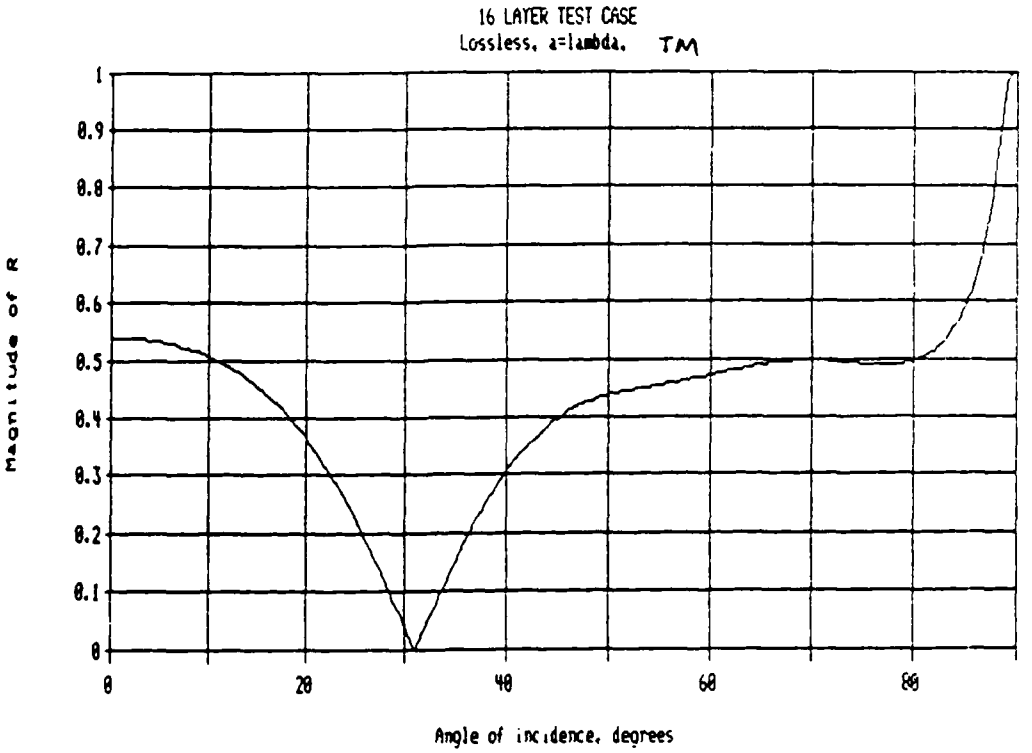
16 LAYER TEST CASE
Lossless, a=lambda, TM
Magnitude of R
1
0.9
0.8
0.7
0.6
0.5
0.4
0.3
0.2
0.1
0
0
20
40
60
80
Angle of incidence, degrees

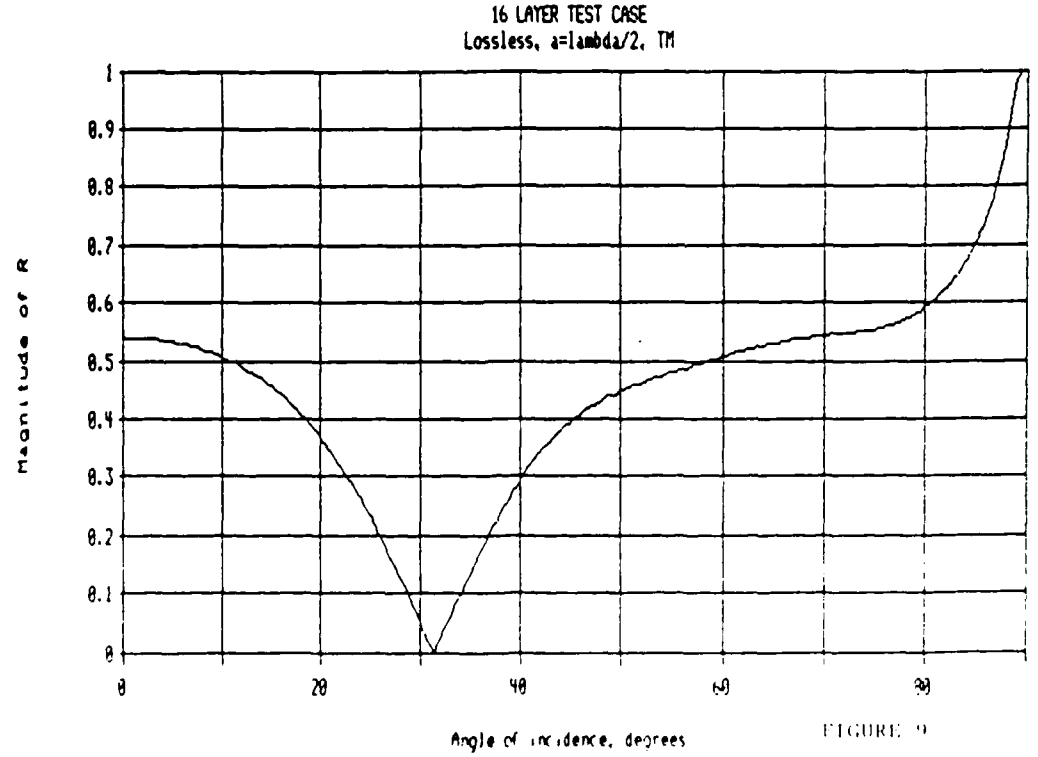
16 LAYER TEST CASE
Lossless, a=lambda/2, TM
Magnitude of R
1
0.9
0.8
0.7
0.6
0.5
0.4
0.3
0.2
0.1
0
0
20
40
60
80
Angle of incidence, degrees

FIGURE 9

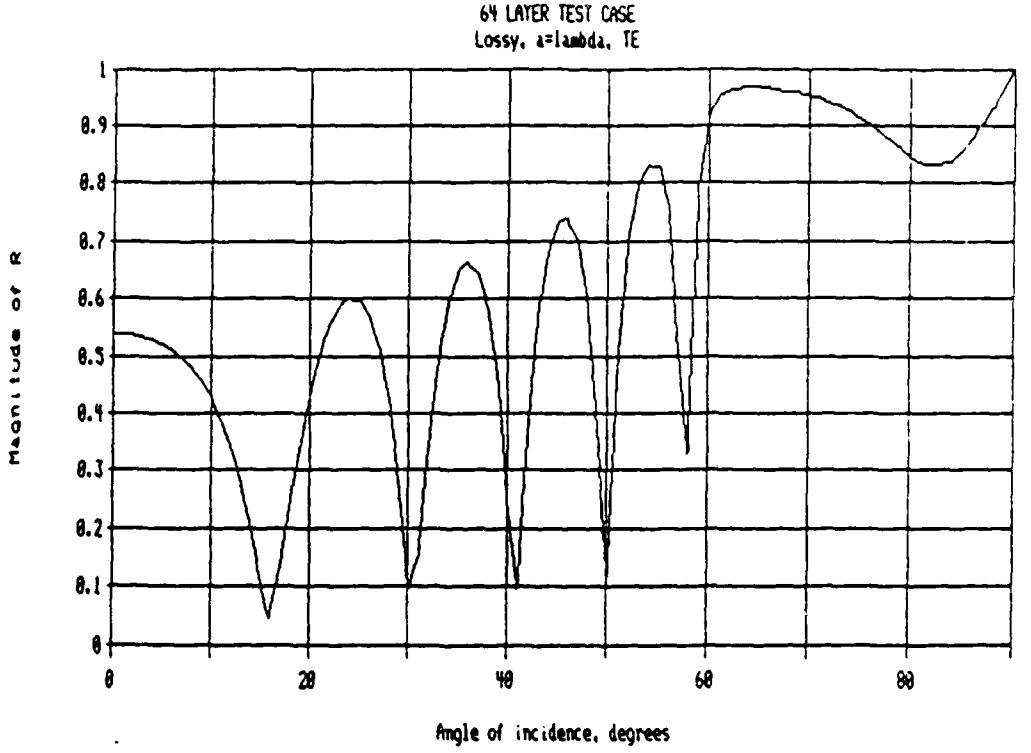
64 LAYER TEST CASE
Lossy, a=lambda, TE
Magnitude of R
1
0.9
0.8
0.7
0.6
0.5
0.4
0.3
0.2
0.1
0
0
20
40
60
80
Angle of incidence, degrees

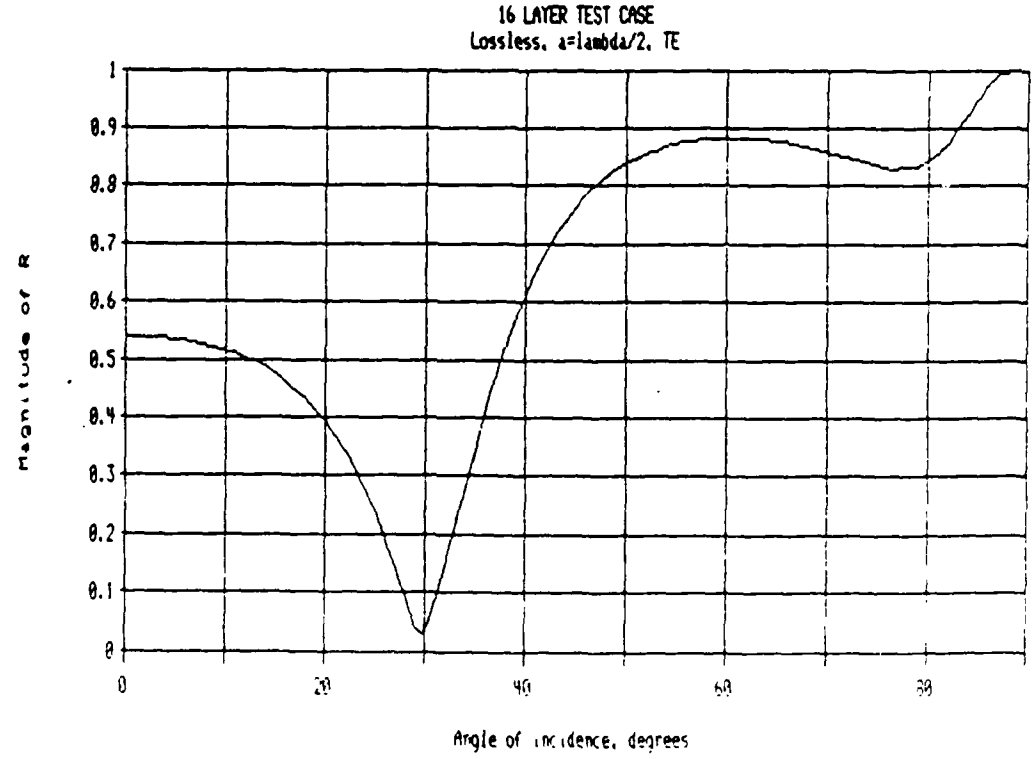
16 LAYER TEST CASE
Lossless, a=lambda/2, TE
Magnitude of R
1
0.9
0.8
0.7
0.6
0.5
0.4
0.3
0.2
0.1
0
0
20
40
60
80
Angle of incidence, degrees

FIGURE 10

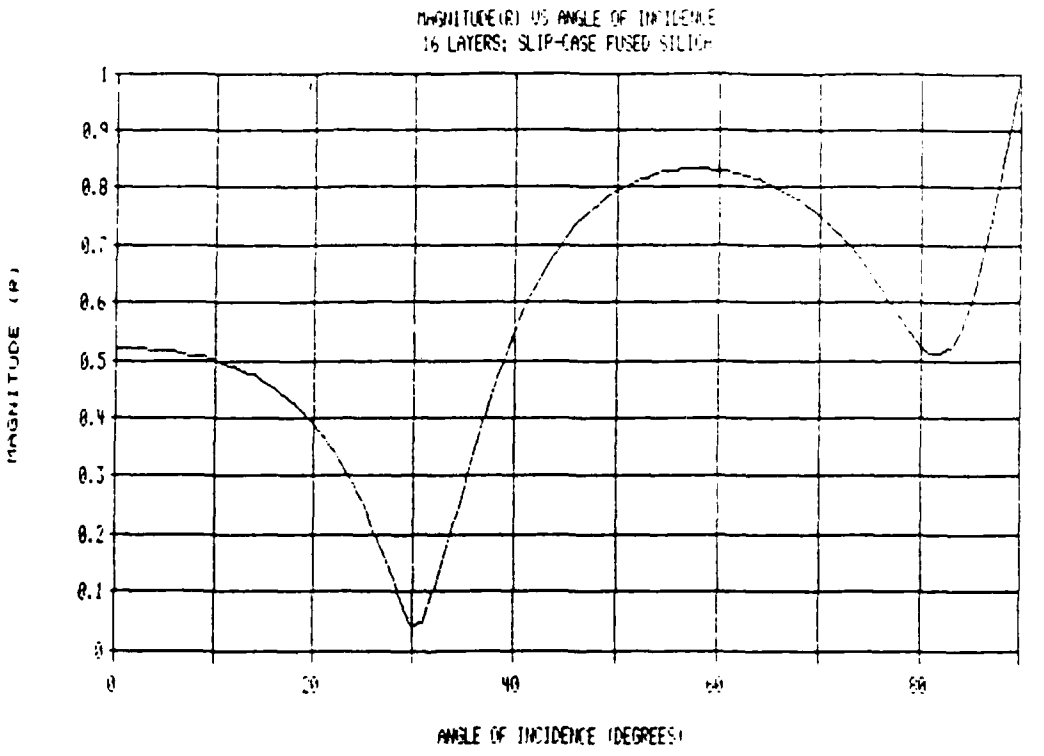
MAGNITUDE(R) VS ANGLE OF INCIDENCE
16 LAYERS; SLIP-CASE FUSED SILICA
MAGNITUDE (R)
1
0.9
0.8
0.7
0.6
0.5
0.4
0.3
0.2
0.1
0
0
20
40
60
80
ANGLE OF INCIDENCE (DEGREES)

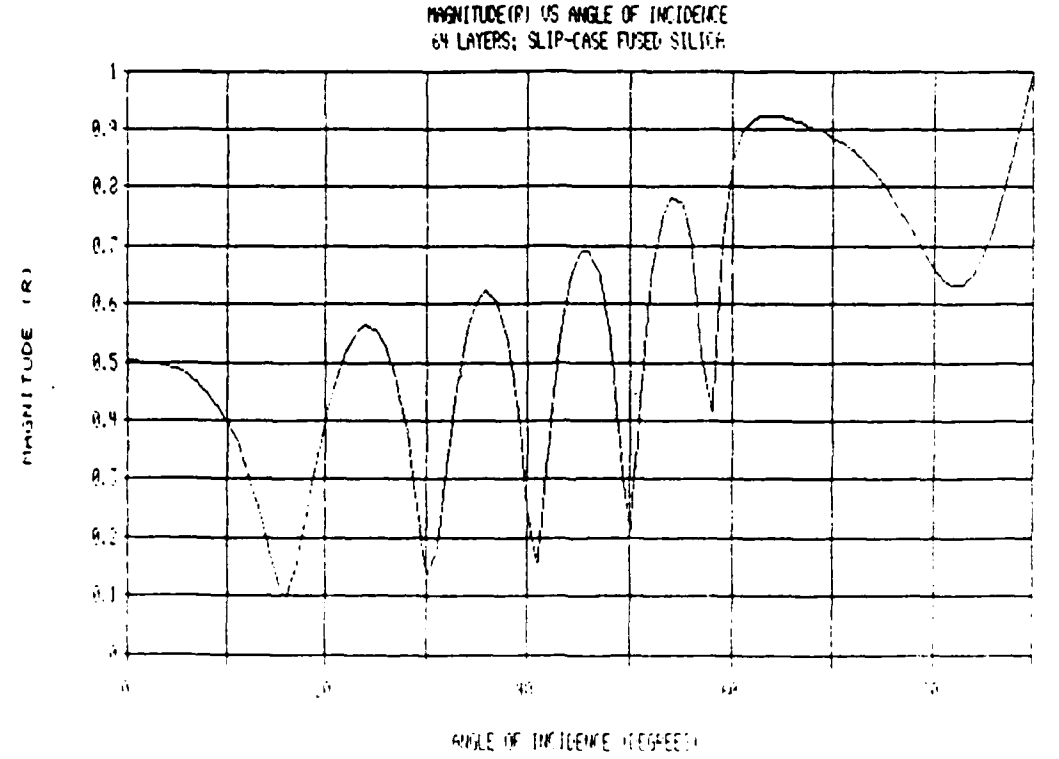
MAGNITUDE(R) VS ANGLE OF INCIDENCE
64 LAYERS; SLIP-CASE FUSED SILICA
MAGNITUDE (R)
1
0.9
0.8
0.7
0.6
0.5
0.4
0.3
0.2
0.1
0
0
20
40
60
80
ANGLE OF INCIDENCE (DEGREES)

FIGURE 11

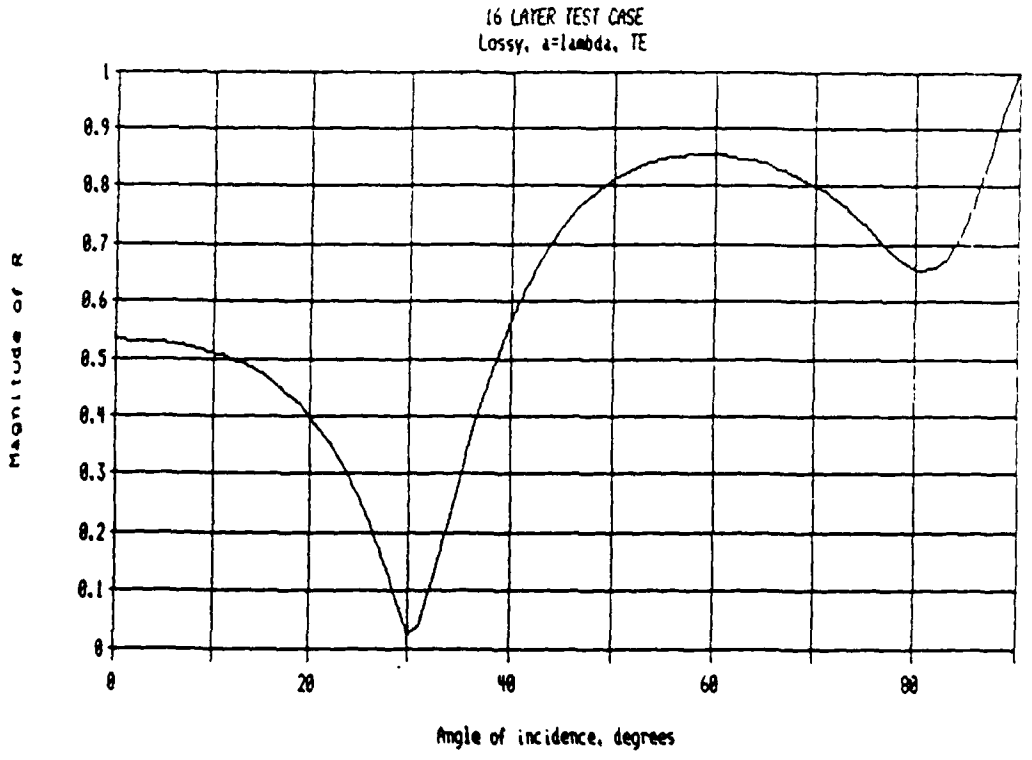
16 LAYER TEST CASE
Lossy, a=lambda, TE
Magnitude of R
1
0.9
0.8
0.7
0.6
0.5
0.4
0.3
0.2
0.1
0
0
20
40
60
80
Angle of incidence, degrees

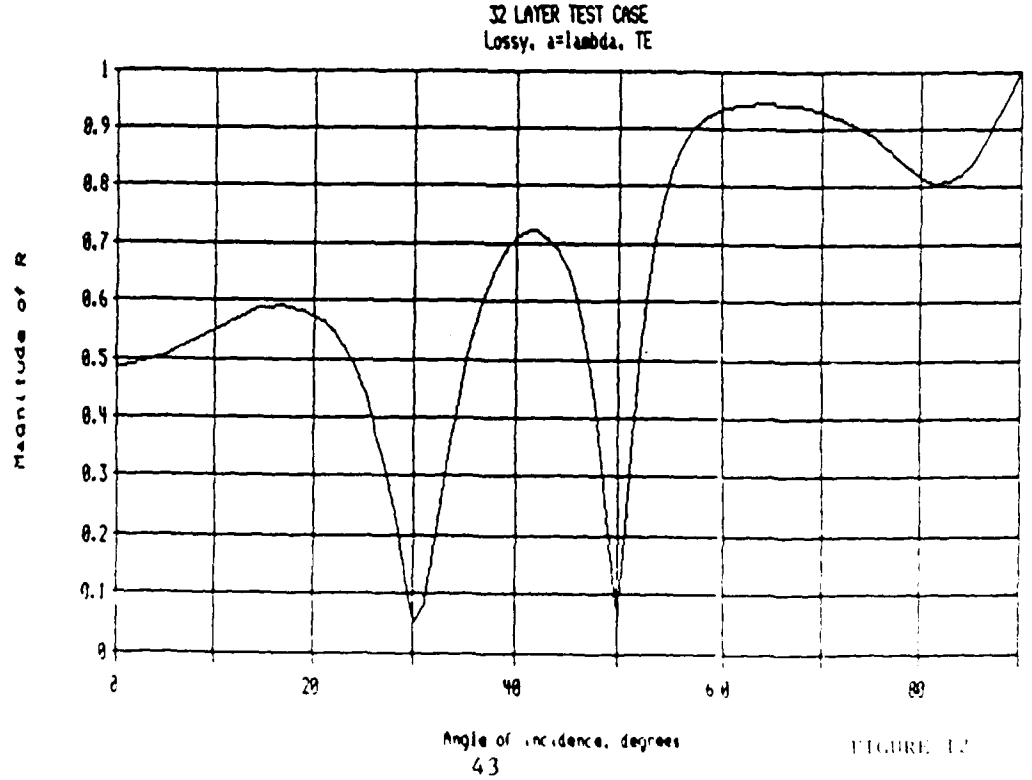
32 LAYER TEST CASE
Lossy, a=lambda, TE
Magnitude of R
1
0.9
0.8
0.7
0.6
0.5
0.4
0.3
0.2
0.1
0
0
20
40
60
80
Angle of incidence, degrees

FIGURE 17

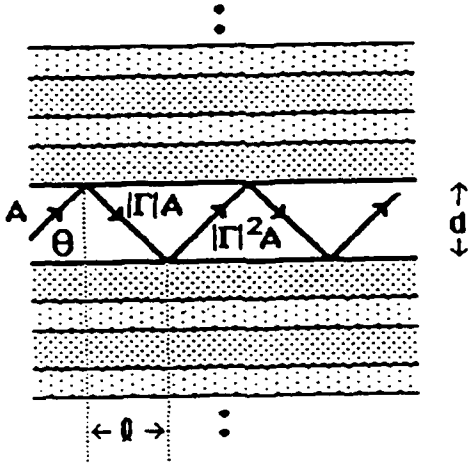

FIGURE 13

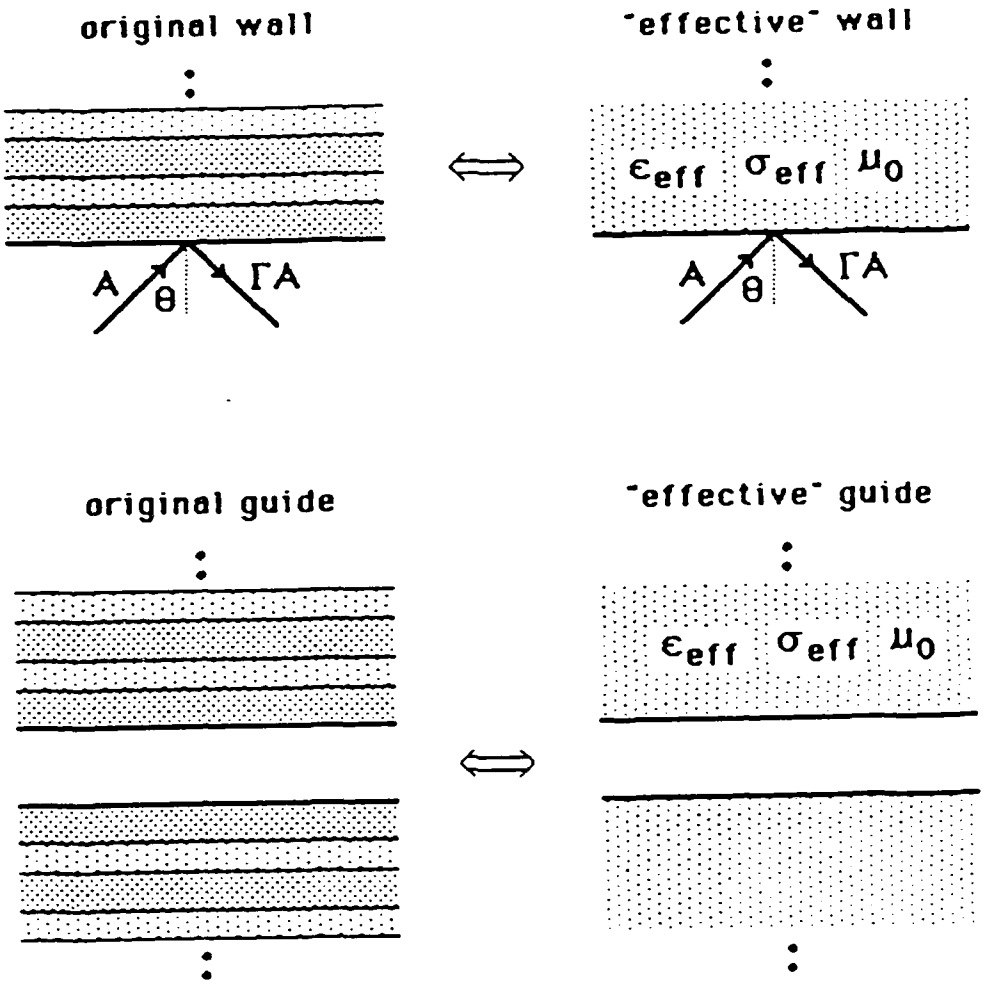
original wall
"effective" wall
ϵ_{eff} σ_{eff} μ_0
A
θ
ΓA
original guide
"effective" guide
ϵ_{eff} σ_{eff} μ_0

FIGURE 14

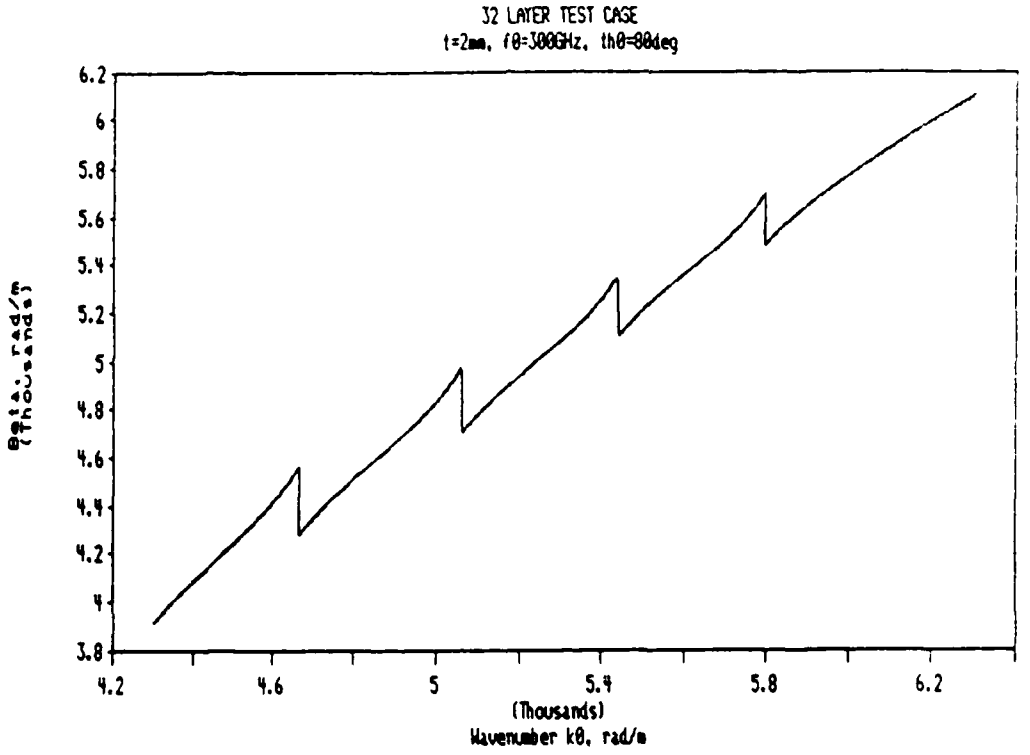
32 LAYER TEST CASE
t=2mm, f0=300GHz, th0=80deg
Beta, rad/m (Thousands)
6.2
6
5.8
5.6
5.4
5.2
5
4.8
4.6
4.4
4.2
4
3.8
4.2
4.6
5
5.4
5.8
6.2
(Thousands)
Wavenumber k0, rad/m

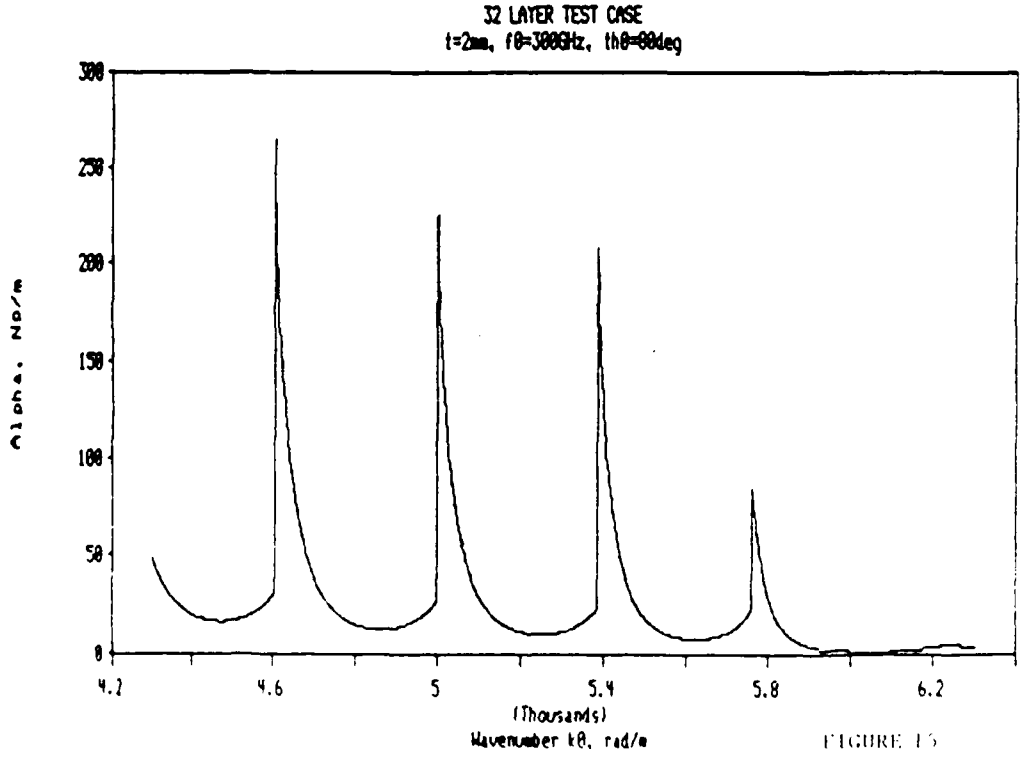
32 LAYER TEST CASE
t=2mm, f0=300GHz, th0=80deg
Alpha, NP/m
300
250
200
150
100
50
0
4.2
4.6
5
5.4
5.8
6.2
(Thousands)
Wavenumber k0, rad/m

FIGURE 15

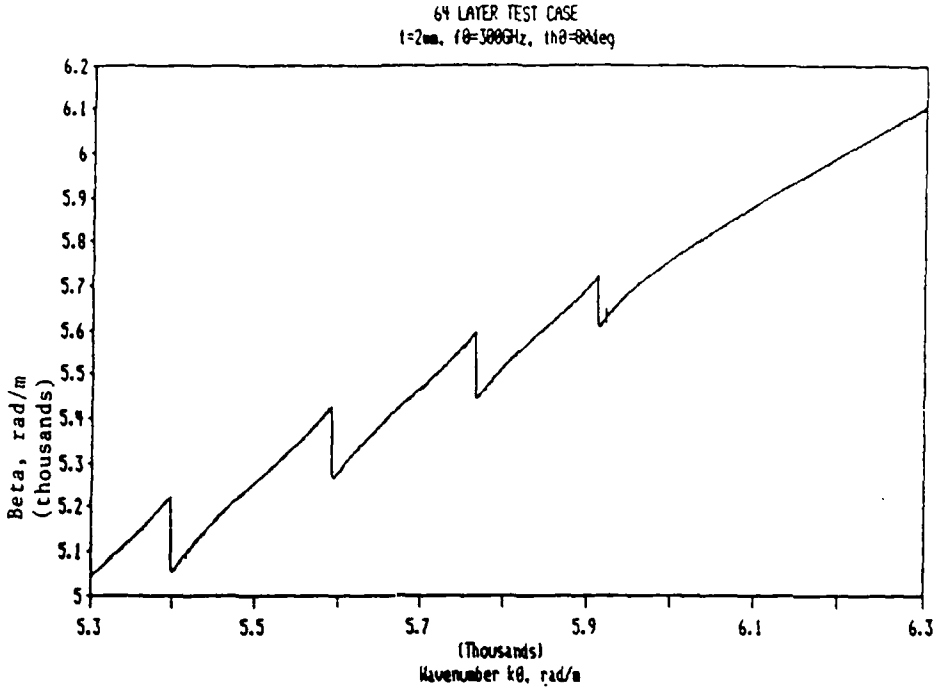
64 LAYER TEST CASE
t=2mm, f0=300GHz, th0=80deg
Beta, rad/m
(thousands)
6.2
6.1
6
5.9
5.8
5.7
5.6
5.5
5.4
5.3
5.2
5.1
5
5.3
5.5
5.7
5.9
6.1
6.3
(Thousands)
Wavenumber k0, rad/m

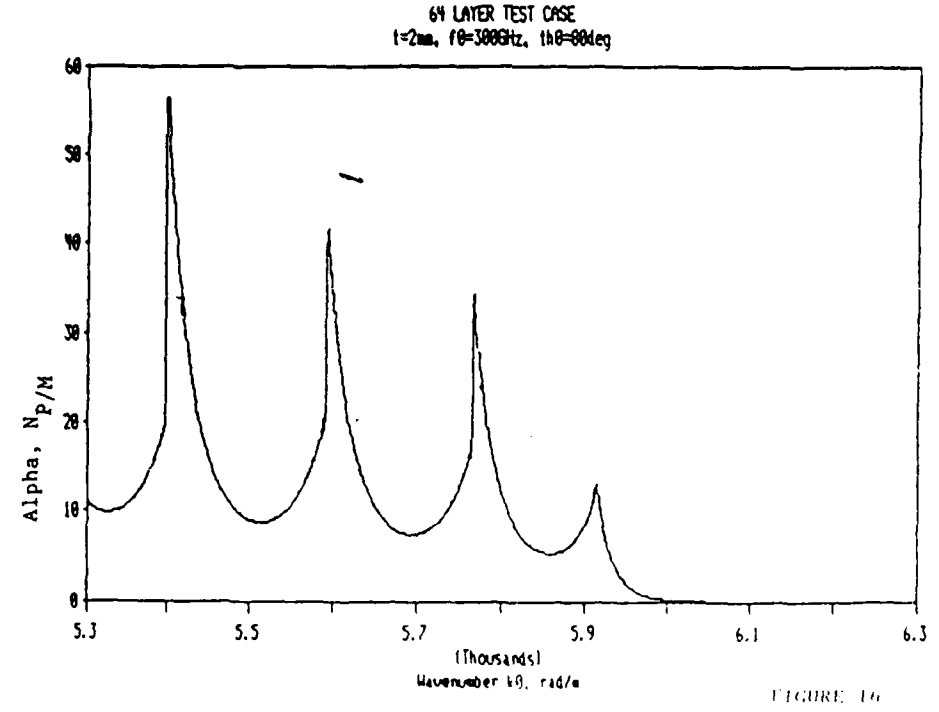
64 LAYER TEST CASE
t=2mm, f0=300GHz, th0=80deg
Alpha, Np/M
60
50
40
30
20
10
0
5.3
5.5
5.7
5.9
6.1
6.3
(Thousands)
Wavenumber k0, rad/m

FIGURE 16

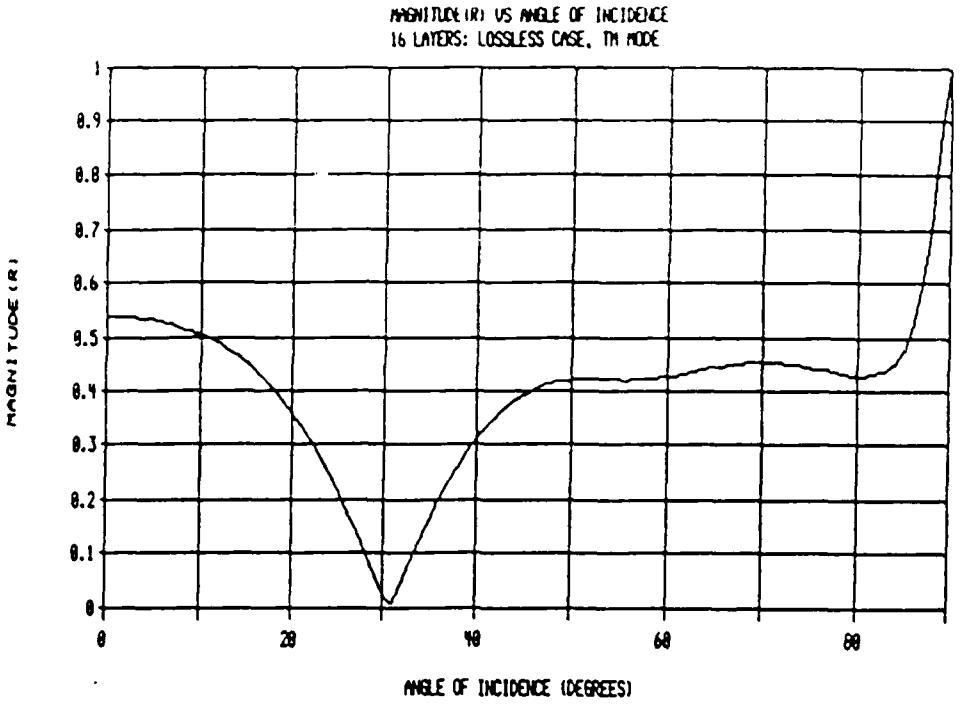
MAGNITUDE(R) VS ANGLE OF INCIDENCE
16 LAYERS: LOSSLESS CASE, TM MODE
MAGNITUDE (R)
1
0.9
0.8
0.7
0.6
0.5
0.4
0.3
0.2
0.1
0
0
20
40
60
80
ANGLE OF INCIDENCE (DEGREES)

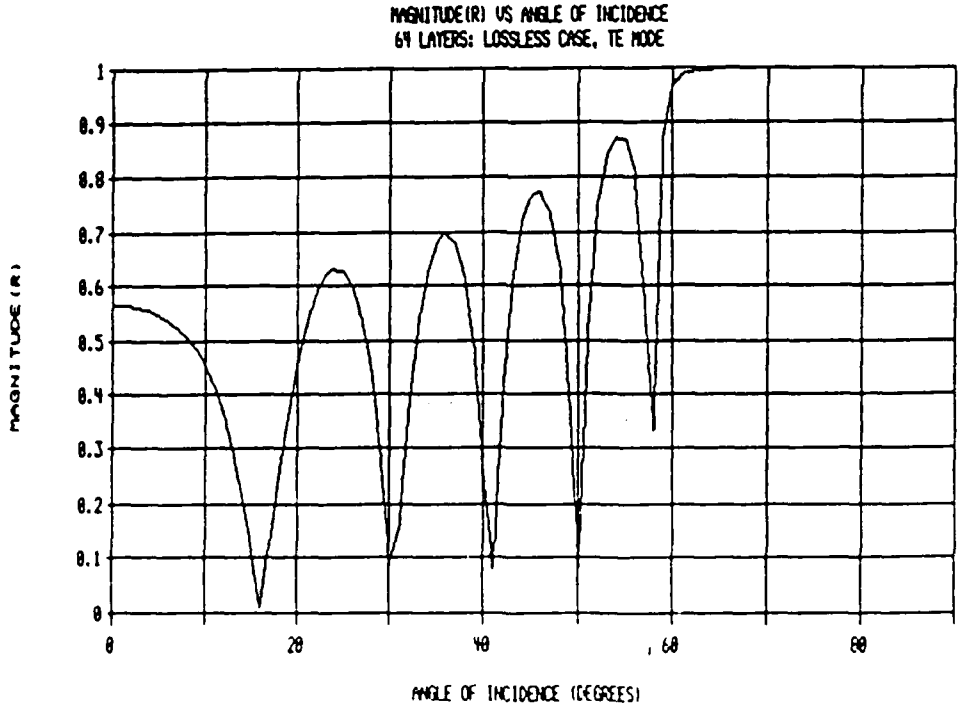
MAGNITUDE(R) VS ANGLE OF INCIDENCE
64 LAYERS: LOSSLESS CASE, TE MODE
MAGNITUDE (R)
1
0.9
0.8
0.7
0.6
0.5
0.4
0.3
0.2
0.1
0
0
20
40
60
80
ANGLE OF INCIDENCE (DEGREES)

Figure 17

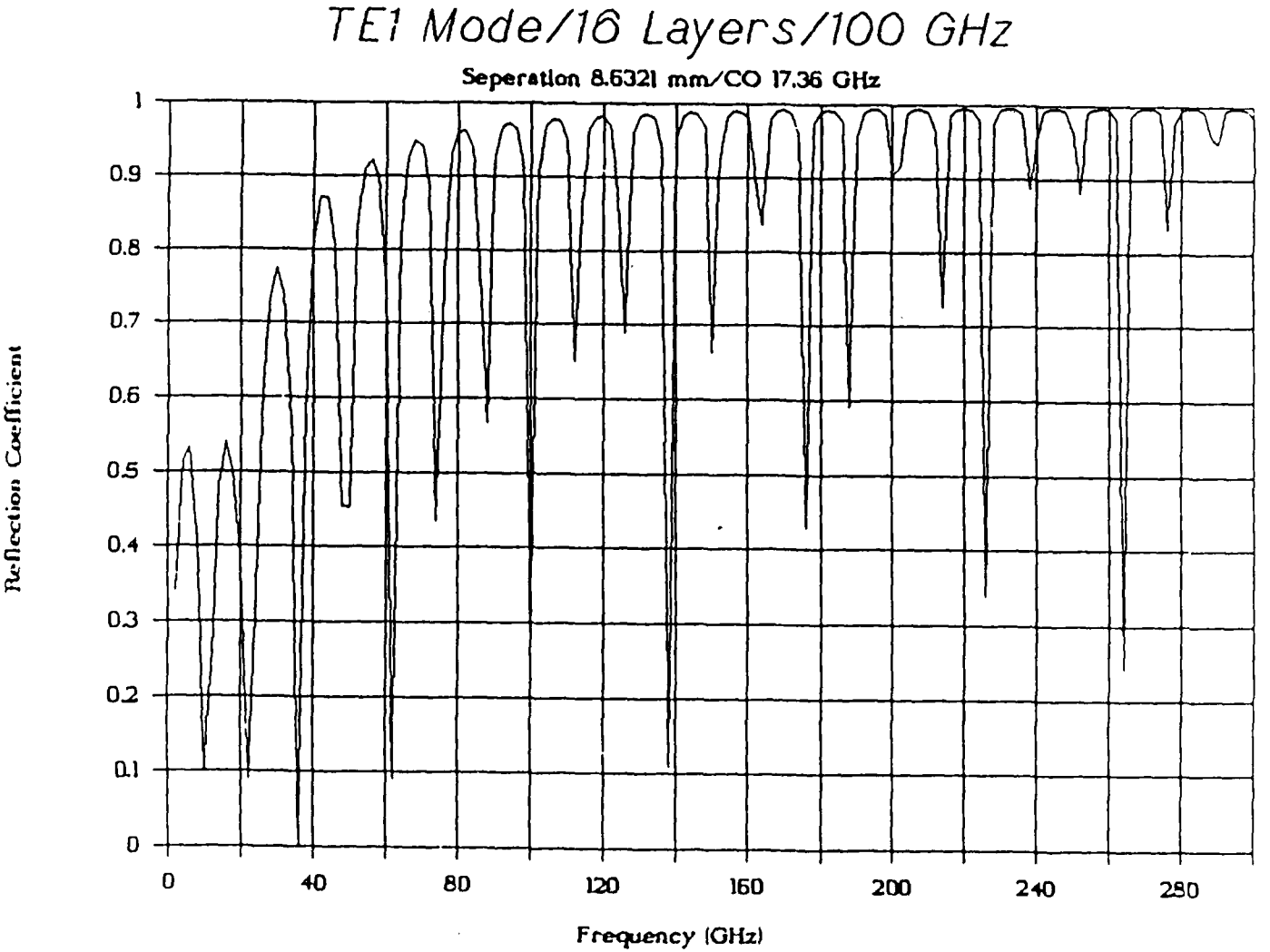
TE1 Mode/16 Layers/100 GHz
Seperation 8.6321 mm/CO 17.36 GHz
Reflection Coefficient
1
0.9
0.8
0.7
0.6
0.5
0.4
0.3
0.2
0.1
0
0
40
80
120
160
200
240
280
Frequency (GHz)

Figure 18

TE Mode – 16 Layers

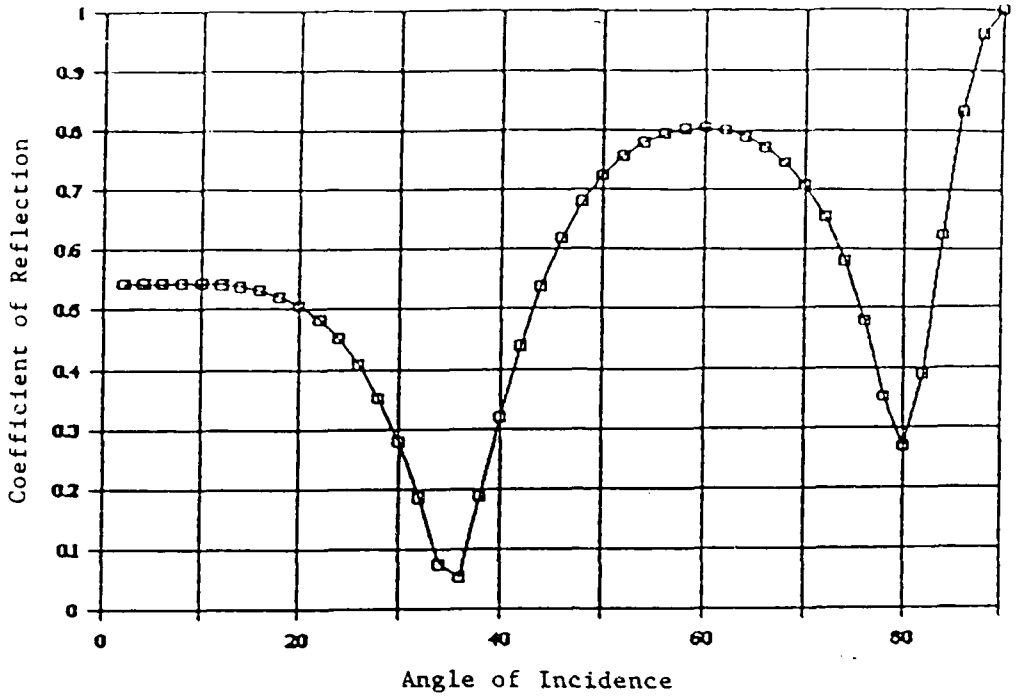

TM Mode – 16 Layers

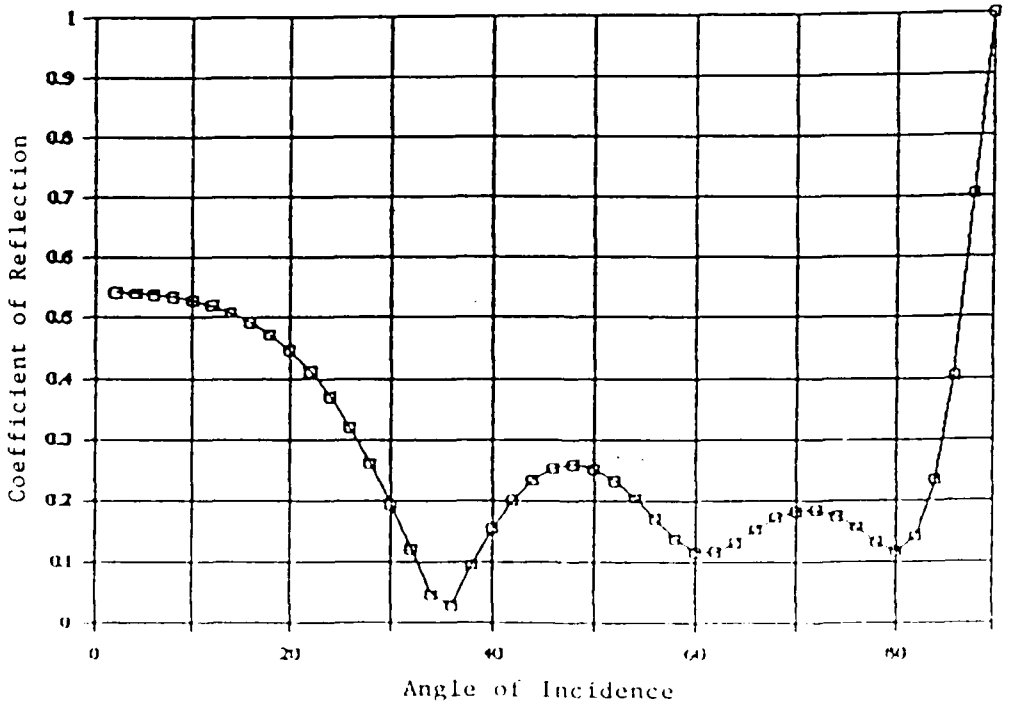

FIGURE 19

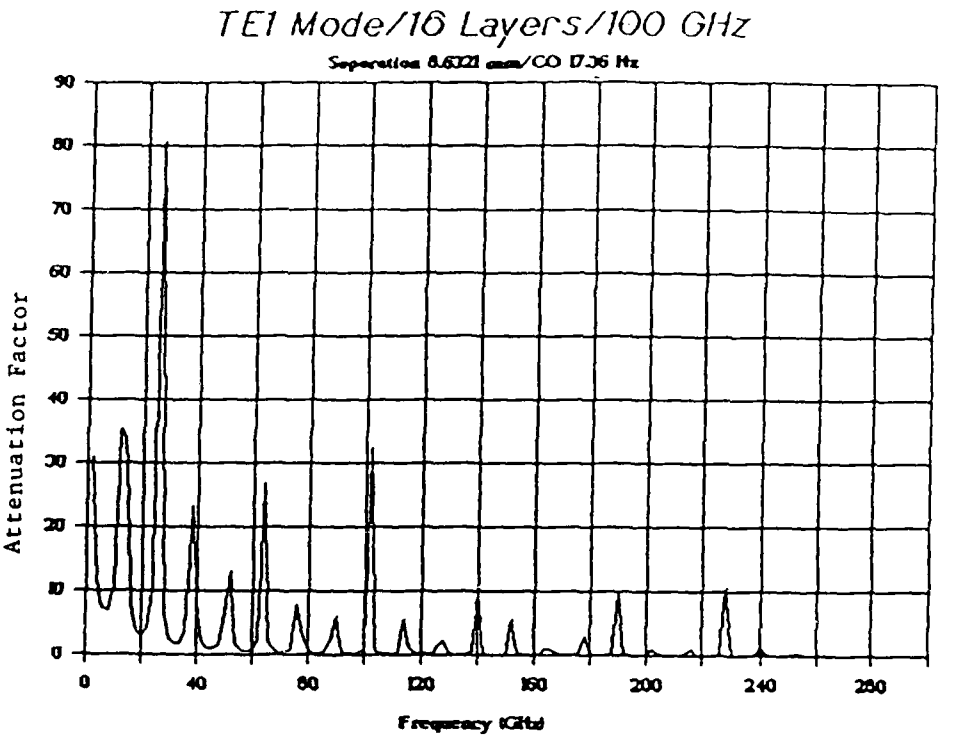
TE1 Mode/16 Layers/100 GHz
Attenuation Factor
0
10
20
30
40
50
60
70
80
90
0
40
80
120
160
200
240
280

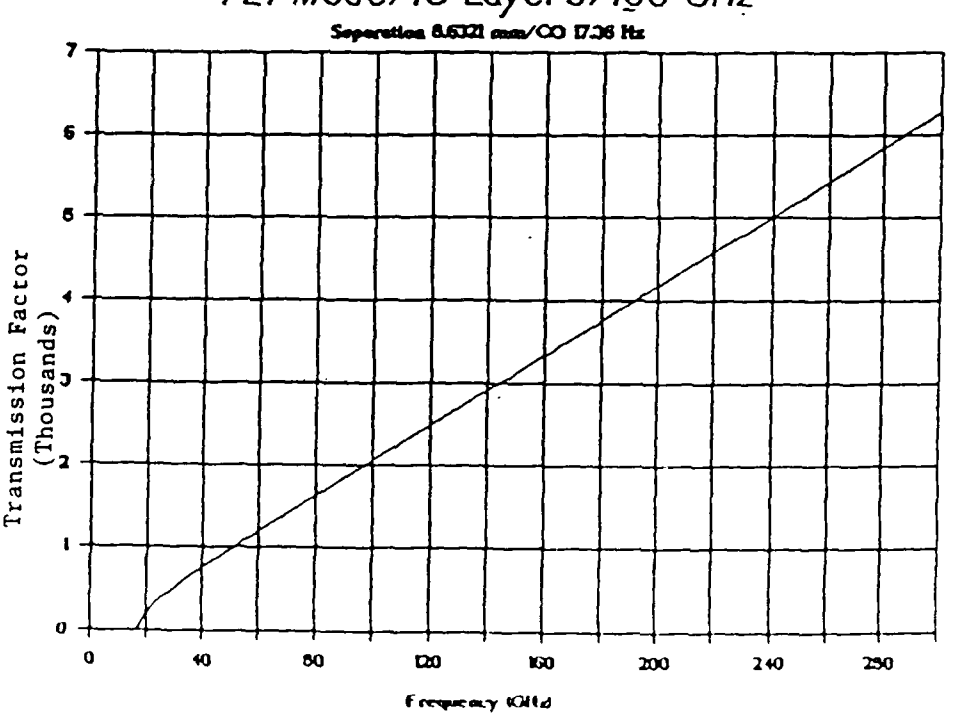
TE1 Mode/16 Layers/100 GHz
Transmission Factor (Thousands)
0
1
2
3
4
5
6
7
0
40
80
120
160
200
240
280

FIGURE 20

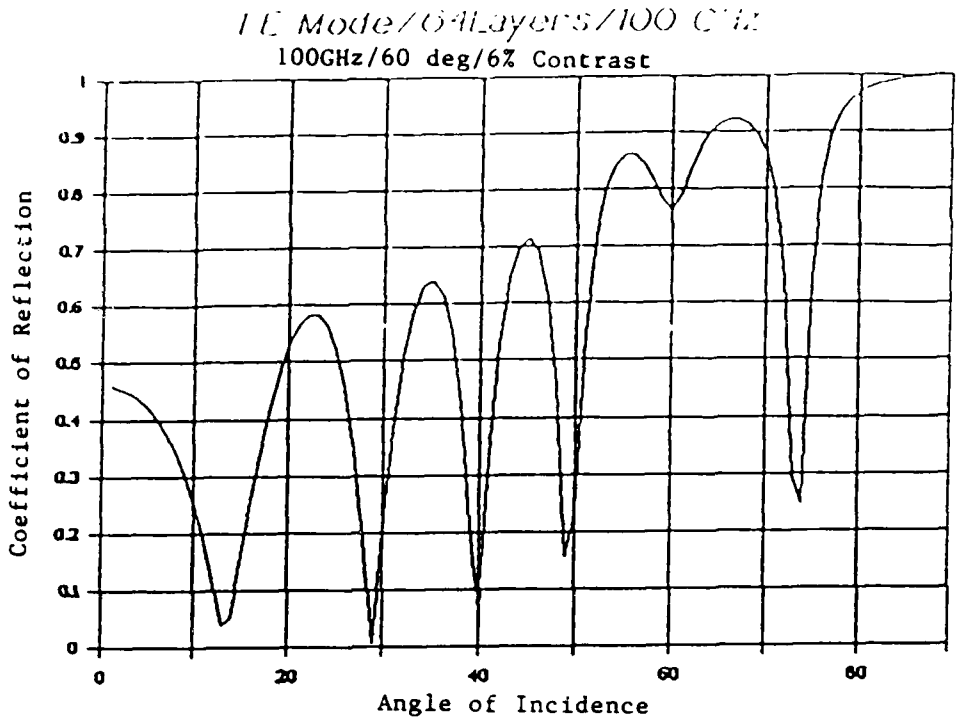
TE Mode/64Layers/100 GHz
100GHz/60 deg/6% Contrast
Coefficient of Reflection
Angle of Incidence
0
0.1
0.2
0.3
0.4
0.5
0.6
0.7
0.8
0.9
1
0
20
40
60
80

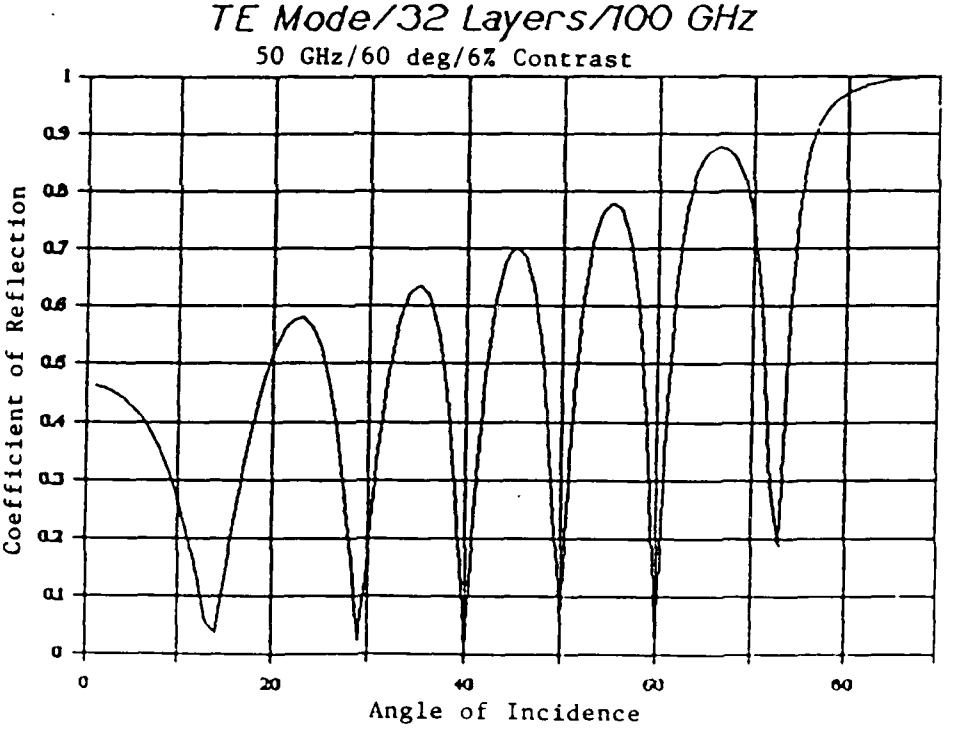
TE Mode/32 Layers/100 GHz
50 GHz/60 deg/6% Contrast
Coefficient of Reflection
Angle of Incidence
0
0.1
0.2
0.3
0.4
0.5
0.6
0.7
0.8
0.9
1
0
20
40
60
80

FIGURE 21

TABLE I

Example: let f=100 GHz, d = 2λ, θ = 88°

α	required $\lvert\Gamma\rvert$
1 dB/m	.980
0.5 dB/m	.990
0.1 dB/m	.998

MISSION
of
Rome Air Development Center

RADC plans and executes research, development, test and selected acquisition programs in support of Command, Control, Communications and Intelligence (C^3I) activities. Technical and engineering support within areas of competence is provided to ESD Program Offices (POs) and other ESD elements to perform effective acquisition of C^3I systems. The areas of technical competence include communications, command and control, battle management, information processing, surveillance sensors, intelligence data collection and handling, solid state sciences, electromagnetics, and propagation, and electronic, maintainability, and compatibility.

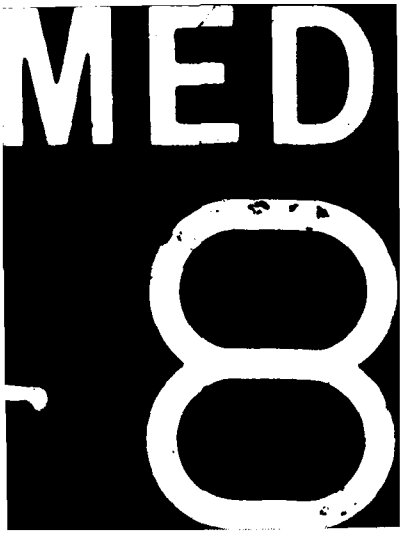
MED
8